Materials Sciences Corporation

NASA CONTRACT REPORT 165753

THERMOMECHANICAL RESPONSE OF GR/PI COMPOSITES

B. WALTER ROSEN, ANIRUDDHA P. NAGARKAR, AND ZVI HASHIN

NASA
National Aeronautics and Space Administration

Langley Research Center
Hampton, Virginia 23665

MSC TFR 1202/0207
MARCH, 1981

DISCLAIMER NOTICE

THIS DOCUMENT IS BEST QUALITY AVAILABLE. THE COPY FURNISHED TO DTIC CONTAINED A SIGNIFICANT NUMBER OF PAGES WHICH DO NOT REPRODUCE LEGIBLY.

Materials Sciences Corporation

THERMOMECHANICAL RESPONSE OF GR/PI COMPOSITES

Technical Final Report
MSC TFR 1202/0207
March, 1981

Prepared by:
B. Walter Rosen, Aniruddha P. Nagarkar, and Zvi Hashin

Prepared for:
National Aeronautics and Space Administration
Langley Research Center
Hampton, Virginia

Gwynedd Plaza II, Bethlehem Pike, Spring House, PA • 215-542-8400

FOREWORD

This report summarizes the work performed by Materials Sciences Corporation (MSC) under NASA Contract No. NAS1-15841. Dr. John Davis was the Technical Representative for the NASA Langley Research Center. The authors express their appreciation to Dr. Davis and to Mr. Gary Farley for their assistance in connection with the experimental data summarized in NASA TP 1867.

TABLE OF CONTENTS

LIST OF FIGURES

LIST OF FIGURES (Continued)

INTRODUCTION

Fiber composite materials are finding applications under increasingly severe load and environmental conditions. Development of polyimide matrix materials has significantly increased the temperature range over which polymeric matrix composites can be used. As a result, the dimensional stability of laminates of such material and the possibility of damage resulting from thermal stresses induced by temperature changes must be considered. A preliminary study conducted to evaluate these problems provided indications that material non-linearity due to high stresses and time dependent material behavior may both have significant influence on the laminate thermal expansion coefficients and on the stress-strain behavior of such laminates. The present program was undertaken to examine these effects for practical laminate configurations subjected to realistic environments.

Determination of the thermoelastic properties of fiber composite laminates on the basis of the thermoelastic properties of the constituting laminae and their stacking sequence is a routine procedure used by composite materials analysts. Even when the thermoelastic properties of the laminae are temperature dependent, the determination of laminate properties is of conventional nature, provided the laminae are elastic at all temperatures. However, unidirectional composites exhibit non-linear behavior when subjected to axial shear stress, or to transverse stress, particularly at elevated temperatures.

In recent years, non-linear mechanical properties of laminates have been successfully incorporated into laminate analysis, primarily in the isothermal case. In the case of Boron/Epoxy and Graphite/Epoxy layers, room temperature non-linearity is exhibited primarily in shear and transverse tension and compression. Room temperature laminate stiffness properties are affected by this non-linearity, but not drastically.

The situation appears to be significantly different in the case of laminates subjected to large temperature changes. This

is due to two phenomena. The first is that non-linear behavior of a unidirectional lamina results from matrix non-linearity which increases significantly with temperature. The second is that large thermal expansion coefficients exist in directions normal to the fibers of a unidirectional laminae. Therefore, as a result of temperature changes, large transverse stresses or strains will be induced even for a fiber-dominated laminate. It is to be expected that non-linearity in the fiber direction can be neglected since the fibers remain stiff and elastic. However, non-linear effects of the stress-strain relation in a direction transverse to the fibers, and in shear, both increase with temperature and have to be considered. Moreover, these transverse and shear effects are not superposable, but are interactive; i.e. the non-linear shear strain depends also on the transverse strain and vice versa. These non-linearities may have a very significant effect upon thermal expansion coefficients even when the effect upon laminate stiffnesses is small.

A procedure for extending the earlier non-linear analysis of mechanical response of laminates to include thermal effects has been outlined in the preliminary study of the present subject area. During the present phase of the program, this procedure has been developed into an automated analysis computer code called TENOL. The analysis procedure treats a general state of plane stress existing in the individual layers of an arbitrary laminate. The individual plies are taken as elastic in the fiber direction and as having a non-linear stress-strain response for loads transverse to the fibers and for axial in-plane shear. These non-linear stress-strain relations are represented by Ramberg-Osgood curves. All material properties are assumed to be temperature dependent. The analysis procedure is described in the following section, "Analysis." A detailed description of the code, including the User's Guide, is presented in an appendix.

The analysis was utilized to study the response of various laminates of graphite and polyimide under conditions of in-plane load and uniform temperature cycles. A complementary experimental

program was performed at the NASA Langley Research Center and experimental results were compared with analytical predictions. This is discussed in the section "Thermal Expansion of Graphite Polyimide Laminates."

Another aspect of material behavior which is of possible importance is the time dependence of the properties of the polyimide matrix. The effects of this are creep deformation and stress relaxation in the laminae of which a laminate is composed. The magnitude of these effects increases with temperature. The internal laminate stresses produced by loads and temperature changes are reduced by stress relaxation; the rate of reduction being dependent on the rate of reduction with time of the relaxation moduli of the laminate at the relevant temperature. It is thus seen that material time dependence is another factor whose importance must be evaluated for stress analysis and design of laminated structures.

A preliminary viscoelastic analysis has been conducted in order to evaluate the relaxation time of a laminate as a function of the relaxation behavior of the unidirectional ply material. Application of this methodology was made for two practical environmental conditions for a quasi-isotropic $[0/\pm45/90]_s$ laminate. First the effect of stress relaxation on the residual stresses due to the fabrication curing cycle was examined, then the effect of stress relaxation on the response of the laminate to thermal cycling representative of the temperature cycles of a satellite in stationary orbit. This material is discussed in the section, "Stress Relaxation in Laminates." Details of the methodology used in the viscoelastic analysis is presented in an appendix to the report.

NON-LINEAR LAMINATE BEHAVIOR

The effects of the non-linearity of unidirectional graphite polyimide upon thermal expansion of laminates have been investigated in a preliminary fashion in reference 1. The non-linear thermal mechanical behavior was modeled in a Ramberg-Osgood form and the non-linear interaction effects between shear stress and transverse stress were taken into account by a generalization of a method developed in reference 2. A general scheme for applying thermal elastic non-linear analysis to laminates was presented. That approach has been utilized herein to develop a general purpose non-linear laminate analysis code for studying combined effects of temperature and membrane loading. The formulation is based upon the following assumptions:

1. At the lamina level, the thermal and mechanical strains are superposable, i.e. the total strain can be obtained by the sum of the free thermal strain and a stress related mechanical strain.
2. The lamina stress-strain relation, though non-linear, is elastic. A 'total' stress-strain relation is written for the orthotropic lamina assuming a state of plane stress.
3. Stress-strain response of the lamina can be approximated by Ramberg-Osgood parameters at different temperatures.
4. All stresses and strains are measured in reference to a stress free state in the laminate at some temperature.

Analysis is restricted to symmetric laminates only. Membrane loads are applied to the laminate. The equilibrium equations, along with the compatibility conditions that the strains in all plies are equal, are used to establish the governing equations. This results in a non-linear set of equations for the ply stresses in terms of the elastic moduli, Ramberg-Osgood parameters, and the applied loads at the temperature of analysis. These

equations are solved using the Newton-Raphson iterative procedure assuming the linear elastic solution as an initial guess.

The coefficient matrix of the system of equations set up at the analysis temperature depends only on the material properties at that temperature and hence, is unique. The solution of this system is also unique. This implies that if a laminate is in a state represented by point A (fig. 1) in the load temperature space, the resulting stress state is independent of the path followed to that point from the reference stress free temperature. Hence, paths 1, 2, and 3 (fig. 1) are equivalent. This formulation can be used to predict the stress state at any point in the load temperature space, hence any load path. Commonly used load paths that can be analyzed and easily verified experimentally are laminate response to a pure thermal load, to a pure mechanical load, to a constant thermal and varying mechanical load, to a constant mechanical and a varying thermal load, etc.

The computer program resulting from this study is described in Appendix A, which also contains a User's Guide for the software.

ISOTHERMAL STRESS-STRAIN CURVES

Stress-strain curves at different uniform temperatures were obtained experimentally by NASA. For comparison, the computer code TENOL was utilized to calculate laminate stress-strain relations based upon various assumptions as to stress free temperature. Although all strains are calculated by the program with reference to 0 strain at the stress free temperature, the results are plotted in the form of difference of strain at the test temperature with 0 load and with each applied load at the same test temperature. This provides for a direct comparison between the analysis and the experiment.

For correlation purposes, calculations were made for a quasi-isotropic $[0/\pm45/90]_s$ and angle plies of $[\pm30]_s$ and $[\pm60]_s$ graphite polyimide laminates subjected to axial tensile loading.

Two different stress free temperatures were utilized in the calculations; room temperature and 316°C. Calculations for the quasi-isotropic laminate are shown in figure 2, along with the experimental results. As indicated, the initial strain at the test temperature has to be subtracted from all of the calculated strains.

The response predicted with both the stress free temperature assumptions is almost linear elastic and correlation between the experimental data and both the predictions is extremely good. The response of the $[\pm 30]_s$ and $[\pm 60]_s$ Gr/Pi laminates predicted has been presented with the experimental results in figures 3 and 4, respectively. The response predicted for each of the laminates is non-linear, and correlates well with the experiments, and the effect of the stress free temperature is negligible. The accuracy of the predicted response, both for linear elastic and non-linear behavior is an encouraging step in the validation of the formulation.

LAMINATE THERMAL EXPANSION

Knowledge of the laminate thermal expansion behavior is essential for the design of space structures for dimensional stability in extreme environments. In an earlier study, (ref. 1) material non-linearity was shown to have significant effects on the laminate thermal expansion coefficient.

When composite laminates are fabricated, individual plies are laid up in the required stacking sequences and the layup is cured at some elevated temperature. At some high temperature and time the laminate is stress free. Subsequent cooling to room temperature results in residual stresses and strains. These stresses relax in time so that the laminate on reheating becomes stress free at some lower temperature. Because of this time dependence, the analysis was conducted assuming two different stress free temperatures. One was assumed to be 316°C, approximately the stress free temperature of a freshly fabricated Gr/Pi laminate, and the

other 24°C, corresponding to significant relaxation of the curing stresses.

In this report, the thermal expansion behavior of Gr/Pi laminates subjected to four different loading conditions was analyzed. They are:

1. Free thermal expansion,
2. Thermal expansion under constant load,
3. Thermal expansion under free thermal cycling,
4. Thermal expansion with thermal cycling under constant load.

Particular attention was given to the effect of material non-linearity and stress free temperature.

Free Thermal Expansion

The axial response of the $[0/90]_s$, $[\pm 30]_s$, and the $[\pm 60]_s$ laminates subjected to a thermal loading was predicted. Results for the two stress free temperatures and test results are presented in figures 5, 6, and 7. These three laminates show different trends. Of interest are the influences of material non-linearity and stress free temperature.

The cross-ply laminate subjected to a pure thermal load has the same thermal expansion characteristics as the $[\pm 45]_s$ laminate or a quasi-isotropic $[0/90/\pm 45]_s$ laminate, hence figure 5 can be used to represent the response of any of these laminates. The shear stresses in this set of laminates are zero, hence the only non-linearity that can affect the response is due to the transverse stress, σ_{22}. Since the stress-strain behavior of the Graphite/Polyimide system transverse to the fibers was found to be nearly linear (fig. 8), non-linear material behavior is not expected to affect the response significantly, as can be seen in figure 5. For a given stress free temperature, the linear elastic prediction and the non-linear prediction from TENOL have very

small differences. This result differs from that of the earlier study, wherein the transverse stress-strain curve showed significant non-linearity.

The stress-free temperature does affect the predictions. For the 0/90 laminate (fig. 5), the effect is on the order of 20%. For this laminate, the experimental result approximates the calculated value for a stress free temperature (SFT) of 24°C within 10%. For most of the temperature range, the experimental result lies between the calculated values for SFT values of 24°C and 316°C.

The $[\pm 60]_s$ laminate behavior (fig. 7) is quite different from that of the cross-ply laminate. This laminate is predicted to have an approximately constant coefficient of thermal expansion over the temperature range from room temperature to 316°C, for both stress free temperature assumptions. The experimental curve also follows the same trend, and lies within approximately 10% of the calculations for SFT = 24°C. However, it does not lie between the two predicted curves. Changing the stress free temperature, however, does affect the thermal expansion in magnitude, but not the trend. The room temperature stress free temperature gives a better correlation with experimental results. The shear and transverse stresses are still small enough for material non-linearity to have no effect.

The $[\pm 30]_s$ laminate response is different from both the $[\pm 60]_s$ and the $[0/90]_s$ laminates. The maximum axial thermal expansion over the whole range is very small compared to the axial thermal response of the $[\pm 60]_s$ laminate. The trends predicted with the two stress free temperatures are the same as those experimentally determined. The material non-linearity has little effect due to the relatively small transverse and shear stresses. Because of the inherently small strain, the change in stress free temperature produces a large percent change in the strain and, hence, in the thermal expansion coefficient. The coefficient is very small up to 191°C when compared to either the unidirectional input or the other laminates.

The code TENOL calculates the correct trends for the free thermal expansion coefficient, or the strain as a function of temperature response, and there is better correlation with experimental data for the analysis assuming a stress free state at room temperature. Percentage differences are not meaningful because of the very low expansion strains. Non-linear material behavior has little or no effect on the material response because of small shear stresses and a low non-linearity in the transverse direction for Graphite/Polyimide.

Thermal Expansion Under Load

In many practical applications, thermal changes take place in a structure subjected to load. Thus, an important problem is the influence of material non-linearity and temperature dependent properties upon the laminate thermal expansion behavior. To study the effects associated with combined loading and temperature change, a series of laminates including $[0/90]_s$, $[0/90/\pm45]_s$, $[\pm30]_s$ and $[\pm60]_s$ were analyzed (see figs. 9-12). Strain response as a function of temperature under applied load was predicted over the temperature range room temperature to 316°C. Calculations utilized the two stress free temperatues used in the free thermal expansion case. Applied stresses of approximately 40% of the design allowables were utilized in the calculations.

For the cross-ply laminate under an axial load, neither the mechanical load nor the thermal load induce shear stresses in the plies. Induced transverse stress in the 90° ply is large, but, since transverse stress behavior shows only a small amount of non-linearity, no significant differences are calculated between the non-linear and the linear elastic solutions. The effect of the stress free temperature is less than 10% which is not as severe as in the free thermal expansion case. As can be seen from figure 9, the experimental data lie between the non-linear predictions of the two stress free temperatures for over 60% of the

temperature range. The predicted room temperature strain values, however, do not match with the experimentally obtained strain. There does not appear to be an obvious explanation for this discrepancy.

In the $[0/90/\pm45]_s$ laminate, an axial load of 159 MPa results in a maximum stress of about 69 MPa transverse to the fibers in the 0° or 90° plies and an 18 MPa shear stress in the 45° plies at room temperature. With the Ramberg-Osgood parameters, σ_y of 207 MPa and τ_y of 86 MPa, these stresses will not cause significant non-linearity. A non-linear analysis at this load level will yield results similar to the linear elastic analysis, as can be seen from figure 12. The effect of the stress free temperature is similar to the case of the free thermal expansion (see fig. 9). Experimental data were not available for correlation.

The $[\pm60]_s$ laminate with a load of 16 MPa was analyzed. The maximum transverse and shear stresses induced are about 48 MPa and 17 MPa, respectively, in the 60° ply, and these are not high enough, even with interaction, to produce any significant non-linear effect. The change in stress free temperature affects the thermal expansion predictions, as can be seen in figure 10, and the experimental data are bounded by the two non-linear predictions. The trend of the laminate expansion is different from that of the cross ply or the quasi-isotropic laminate.

The next case analyzed was the $[\pm30]_s$ laminate under a constant axial load of 105 MPa. At 316°C, even though the transverse stress is predicted to be only about 21 MPa, the maximum shear stress is predicted to be about 17 MPa. With the τ_y of 20 MPa, non-linear effects due to shear are significant, as can be seen from figure 11. The 316°C stress free temperature predictions of the non-linear and linear elastic behavior are quite different, due to the non-linear and temperature dependent behavior of the Graphite/Polyimide. The experimentally observed strain is within the two stress free temperature predictions over about 2/3 of the analysis range, but is different from either prediction at room temperature.

The thermal expansion curves under load are generally in the range of the analytical calculations, with the most pronounced discrepancy being the differences between calculated and experimental values of strain at room temperature resulting from the application of load on the $[\pm 30]_s$ and on the $[0/90]_s$ laminates. No explanation exists for this discrepancy. It should, however, be noted that the stress-strain curve obtained from a test of a $[\pm 30]_s$ laminate at room temperature (described earlier) gave a strain much lower than the reported strain in the experiment described in this section.

In addition, it should be noted that whereas the free thermal expansion curves were generally in good agreement with the calculations based on a stress free temperature equal to room temperature; here, for certain laminates under load, the agreement is better with the assumption of a 316°C stress free temperature.

It should also be noted that transverse stress-strain curves for the basic unidirectional ply material were generally nearly linear to failure. Ramberg-Osgood stress-strain curves were fitted to these transverse stress-strain data using a least squares fit and no terminating strength value was introduced to the curve. If calculated tension stresses were in excess of the material strength of 69 MPa (a condition which can exist in laminates - particularly when there is a relatively high stress free temperature), the stress-strain representation that was used would be in error. In general, it would be reasonable to expect in-situ microcracking for transverse stresses greater than the ply strength. Such an accumulation of microcracks could result in an apparent non-linear transverse stress-strain behavior, which was not modeled by the present analysis.

THERMAL CYCLING

Space structures, such as geostationary satellites, undergo thermal cycling with the temperature changing from 316°C during

the day to -157°C at night. Laminate response to cyclic loading is, therefore, of interest. This part of the report deals with the thermal expansion behavior of composite laminates subjected to thermal cycling. Analyses were conducted for free thermal expansion and expansion under load. There is an inherent problem in conducting these analyses. Cycling requires the inclusion of residual stresses in the formulation. If the analysis is based on an incremental stress-strain relation, the inclusion of residual stresses is a relatively straightforward procedure. The code TENOL, used for the analyses in this report, is based on a total stress-strain relation. Such a formulation is path independent, the stresses and strains being calculated from compliances at the final state of load and temperature, regardless of how that state is reached. Hence, at a given state of load there is a unique state of stress. In cycling in the presence of inelastic behavior, the stresses and strains for a given load state depend on the path. So inherently, a total stress-strain formulation based analysis cannot be used to predict cycling response in the presence of any inelastic behavior. Here, a cyclic load analysis is simulated by two separate analyses: one linear elastic, and the other non-linear. The linear elastic analysis is translated appropriately to present the unloading phase of the load cycle. Laminate response for thermal cycling with and without load was predicted.

Free Thermal Cycling

A $[\pm 45]_s$ laminate was chosen for the analysis. The results of the non-linear and linear elastic analysis are presented in figure 13 for stress free temperatures of 316°C and room temperature. It can be seen that there is little difference in the thermal expansion behavior due to non-linear behavior (this was observed earlier for the $[0/90]_s$ laminate which has the same free thermal expansion characteristics). Therefore, if the stress

free temperature is constant, the analysis predicts little or no hysteresis. For these assumptions, the thermal expansion coefficient remains the same when heating or cooling.

It should be noted that the magnitude of total free thermal strain between any two temperatures may depend upon the value of the stress free temperature (e.g. figs. 5, 6 and 7). Thus, if there is a change in SFT after a cooling cycle, a subsequent reheating cycle will not produce the same total strain change as the initial cooling cycle. If the assumption is made that the stress free temperature varies during the heating and cooling phases of the cycle, the analysis predictions will depend upon such changes. The thermal expansion response of the $[\pm 45]_s$ laminate for different stress free temperatures appropriately translated is different even for linear elastic behavior. Thus, a change in the stress free temperature during the thermal cycle would result in an apparent hysteresis. This is demonstrated in figure 14. Here it is assumed that a heating cycle is conducted starting with a SFT = 24°C. If the stresses relaxed after such a cycle, the subsequent cooling cycle would result in the strain vs. temperature curve shown for SFT = 316°C (translated to match the initial 316°C calculation).

THERMAL CYCLING UNDER LOAD

As was shown earlier, the thermal expansion characteristics of Gr/Pi laminates are affected by material non-linearity to a varying degree, dependent on the magnitude of the induced shear stress. A $[\pm 45]_s$ laminate, when axially loaded, represents a stress state of almost pure shear. Therefore, material non-linearity can be expected to significantly affect the laminate response. The thermal expansion response of a $[\pm 45]_s$ laminate loaded axially with σ_x = 34 MPa was predicted using TENOL (fig. 15). Due to the large mechanical strains, the effect of changing the stress free temperature can be neglected. The linear

elastic response is quite different from the non-linear prediction, the difference increasing at higher axial loads. In the heating cycle, the laminate is losing its stiffness and also becoming more non-linear as the temperature increases. Note that for the $[\pm 45]_s$ laminate, the non-linear calculation shows a monotonically increasing curve of strain with temperature. This is quite distinct from the thermal expansion without load, in which the thermal strain increases and then decreases. In view of this, the agreement between experiment and analysis for the heating portion of the cycle is good. There is a question as to what analysis should be used during the cooling cycle. The argument can be made that since the strains are decreasing due to a stiffening of the material as the temperature comes down, that this unloading analysis should be an elastic analysis. That is the basis for the calculated value shown in figure 15.

There are two discrepancies between analysis and experiment during the cooling cycle. First of all, there was a significant amount of strain taking place at the 316°C temperature before the cooldown started. This is not accounted for in the analysis. For the experiment, it is assumed to be a time dependent strain rather than any non-linearity associated with stress. The second difference is that, on cooling, the experiment showed essentially no change in strain during the cooldown cycle and the analysis shows a strain reduction during that cycle. It is also possible that there are time dependent phenomena influencing the entire cooldown cycle, but that is speculative.

VISCOELASTIC ANALYSIS OF GRAPHITE/POLYIMIDE LAMINATES

When composite laminate structures are utilized in extreme thermal environments there exists the possibility of time dependent response of the material. In general, the matrix material is the source of the time dependent response. The fibers are generally elastic. This results in a unidirectional lamina which will be elastic in the fiber direction and perhaps viscoelastic in the transverse direction. The importance of this behavior will increase at elevated temperatures, particularly near or above the matrix glass-transition temperature. The present study was directed toward an evaluation of the influence of such time dependent behavior upon the laminate response. Creep deformation and stress relaxation are results of this time dependence. One problem that needs to be addressed is predicting behavior of a laminate given the time dependence of the unidirectional laminae, particularly the relaxation time. Another is the laminate response to thermal cycling. The following section deals with these problems.

STRESS RELAXATION IN LAMINATES

The purpose of this analysis is to predict the characteristic relaxation time of a laminate given the relaxation behavior of the unidirectional material. Since this report deals with laminate response to thermal loads, the stress relaxation behavior of the thermally induced curing stresses is analyzed. A methodology has been developed and demonstrated with a sample analysis. Certain simplifying assumptions were made to obtain a closed form solution. The methodology followed is to express the plane stress equations in a time dependent form and apply lamination theory in the Laplace transformed plane. The appropriate constitutive relation has to be used to describe the material behavior, and is usually obtained from curve fitting the experimental data for the material. A quasi-isotropic laminate has been used to demonstrate the analysis procedure.

A quasi-isotropic laminate subjected to a pure thermal load has a very simple state of strain due to various symmetries. In a laminate (fig. 17) the strains in any layer are given by:

$$\varepsilon_{ij}(t) = \varepsilon(t)\delta_{ij} \; ; \; i,j = 1,2 \tag{1}$$

where δ_{ij} is Kronecker delta.

Since there are no shear strains present in the orthotropic laminae, there are no shear stresses. The viscoelastic effects, therefore, are primarily due to the stresses transverse to the fibers. It is assumed that there is no viscoelasticity in the fiber direction, nor for the associated Poisson's effects. Stress-strain relations for a layer, with the stress constant in time are:

$$\varepsilon_{11} = \frac{\sigma_{11}}{E_A} - \frac{\nu_A}{E_A}\sigma_{22} + \alpha_A(\phi_o - \phi_c) \tag{2}$$

$$\varepsilon_{22} = -\frac{\nu_A}{E_A}\sigma_{11} + \frac{\sigma_{22}}{E_T} + \alpha_T(\phi_o - \phi_c) \tag{3}$$

where:

ϕ_o - analysis temperature

ϕ_c - stress free temperature.

The beginning of the relaxation process is defined to begin at time equal to zero at room temperature ϕ_o. The elastic moduli E_A and ν_A can be assumed to be constant, and the only time dependent modulus to be E_T. The plane stress relations can then be transformed into the viscoelastic relations using hereditary integrals, and they become:

$$\varepsilon_{11}(t) = \frac{\sigma_{11}(t)}{E_A} - \frac{\nu_A}{E_A}\sigma_{22}(t) + \alpha_A \Delta\phi H(t)$$

$$\varepsilon_{22}(t) = -\frac{\nu_A}{E_A}\sigma_{11}(t) + \ell_T(t)\sigma_{22}(0) + \int_0^t \ell_T(t-\tau)\frac{d\sigma_{22}}{d\tau}$$

$$+ \alpha_T \Delta\phi H(t) \qquad (4)$$

where H_T is the Heaveside unit step function.

They can be reduced to linear equations by applying Laplace transform. Due to various symmetries, in the $[0/\pm45/90]_s$ laminate, there is only one stress. This stress is determined by lamination theory in terms of E_A, ν_A, ℓ_T. These calculations have been presented in Appendix B, and the resulting expression for the transverse stress in any layer is given by:

$$\hat{\sigma}^k_{22} = -\Delta\phi \frac{E_A(\alpha_T - \alpha_A)}{1 + 2\nu_A + \frac{E_A}{E_T}} \times \frac{1}{s + \frac{E_A/E_T}{1 + 2\nu_A + E_A/E_T} \times \frac{1}{t_r}} . \qquad (5)$$

To be able to calculate inverse transform of this equation and obtain a closed form solution for the stresses, a simple Maxwell behavior for the material is assumed; i.e.:

$$\varepsilon_{12} = \frac{\sigma_{22}}{E_T} + \frac{\sigma_{22}}{\eta_T} \tag{6}$$

the characteristic relaxation being:

$$t_r = \frac{\eta_T}{E_T} . \tag{7}$$

The stress $\hat{\sigma}^k_{22}$ can then be backtransformed to yield the characteristic time t^*_r for the laminate to be (from Appendix B):

$$t^*_r = t_r\left(1 + \frac{E_T}{E_A} + \frac{2\nu_A E_T}{E_A}\right) . \tag{8}$$

The stresses in the laminate therefore relax slower than those in the unidirectional laminae.

The above analysis is at an elementary level. The material behavior can be expected to be more complex than the simple Maxwell type assumed. Hence, the lamination theory solution for the stress σ^k_{22} is likely to be of a form that cannot be inverted easily or exactly, and some approximate numerical technique will have to be used. Variation of σ^k_{22} in time has then to be plotted and the characteristic time determined. A simpler inversion technique can be used with a quasi-state assumption, as done by Kibler (ref. 3). The present analysis is a demonstration of the analysis procedure for the simplest case possible.

VISCOELASTIC RESPONSE TO THERMAL CYCLING

The significance of material viscoelasticity in the response of a composite space structure subjected to daily temperature cycles has been treated as an example of this effect. Thermal strain was evaluated for an environment in which the temperature changed from -157°C to 316°C and back to -157°C in a period of one day. Here again, the simplest case was chosen to demonstrate the analysis procedure. The procedure used was developed in reference 4, and was adapted for the present program.

A cross-ply laminate subjected to a purely thermal load was analyzed. There are no shear stresses induced in the laminate due to the loading, and the material behavior in the fiber direction is assumed to be elastic. The viscoelastic laminate response is due to behavior transverse to the fibers. The expansion coefficients α_A, α_T, and the modulus in the fiber direction E_A are assumed to be constant. An elastic solution for the stress σ_2 is:

$$\frac{\sigma_2}{(\alpha_A-\alpha_T)} = \frac{E_T \Delta\phi}{1 + \frac{E_T}{E_A(1+2\nu_{12})}} . \qquad (9)$$

The behavior of E_T in time has to be known throughout the temperature range. This is achieved in a compact form for a thermorheologically simple material by shifting the compliances at various temperatures and times. The analysis is then conducted by defining a reduced time parameter with a time temperature shift factor and a compliance master curve (refs. 5,6). The relaxation process is assumed to occur quasi-statically so that the compliance is a simple reciprocal of the modulus. This static equation can be written in the form of a heriditary integral, and that integral evaluated by direct integration numerically using the

time/temperature shift factor and the compliance master curve. The resulting equations can be found in Appendix C.

The principal difficulty in the analysis was the lack of experimental data for Graphite/Polyimide. Master curves and shift factor for Graphite/Epoxy were available from two sources (refs. 3,7). The master curves from tests by Brinson (ref. 7) extended over a somewhat larger range and were extrapolated and used (fig. 18). Two different shift factor curves (fig. 19), one of them from reference 7, were used and the laminate cycled in those temperature ranges. Numerical integration was carried out assuming a constant rate of change of temperature in all the cases analyzed.

The higher shift factor (b=.071) corresponds to a greater viscoelastic behavior. When the laminate is cycled between -18°C and 177°C (fig. 20) at the highest temperature, the maximum stress (relative to -18°C) is not as large as the linear elastic prediction and at the end of one complete cycle there is a residual stress. This stress increases slightly in the next cycle. There is little difference between the two shift factor predictions. When the range of the cycling is between -73°C and 204°C, however, the two predictions begin to show a small difference (fig. 21). The residual stress at the end of the first cycle is larger and grows faster at the end of each cycle than in the lower temperature range. The maximum stress also is not as large, due to some relaxation at high temperature (fig. 22).

When the range of the cycling is extended from -157°C to 232°C, there is significant relaxation behavior and at the end of the first cycle a large residual stress is predicted. The maximum stress also is much smaller than the linear elastic prediction and though the trend in the predictions of the two shift factor assumptions is the same, there is a difference in the magnitude predicted.

Such a prediction of the stress is translated into a strain temperature plot and presented in figure 23. It is qualitative in nature because of the uncertain material properties, as is most of this analysis. Let us consider the cross-ply laminate being cycled between -157°C and 316°C. The assumption of constant α_A, α_T and moduli would predict a strain response between ε_1 and ε_2 for all cycles in a linear elastic prediction. Since the unidirectional material is viscoelastic at higher temperatures, there will be some stress relaxation and the stress magnitude and hence the strain will be less than the linear elastic prediction. In the cooling part of the cycle, at the higher temperature there is still some viscoelastic behavior; however, below a certain temperature, these effects are not as significant and the predicted response will be parallel to the linear elastic prediction. This results in a larger strain at -157°C than at the beginning of the cycle. This behavior is repeated in the next cycle, and the maximum stress and strain are smaller and the strain at -157°C even larger. Such a behavior would suggest that there will be very small stresses at the higher temperature and a shift of the range over which the strains vary. A laminate which is initially cycled over a temperature range causing strains of $+\varepsilon_1$ and $-\varepsilon_2$ will approach a steady state solution of cycling between strains of 0 and $\varepsilon_1 + \varepsilon_2$. This will affect the dimensional tolerances and the way they are specified in the design for such a structure. Even though this conclusion is based on Graphite/Epoxy properties, and an elementary analysis, it is valid for any composite laminate made from a constituent material that has significant viscoelastic behavior in the range of the thermal cycling.

DISCUSSION

The basic concern associated with stress dependent non-linearity was that the matrix dominated stress-strain relations of the unidirectional laminae could be expected to be non-linear to a significant degree. This expectation was supported by preliminary experiments conducted in an earlier program (ref. 1). However, in the present study it was found that the current samples of the material, although showing significant non-linearity when subjected to shear stresses, did not show any significant non-linear behavior when subjected to stresses transverse to the fiber direction.

It should be noted that there can be differences between lamina stress-strain behavior obtained from unidirectional material, as opposed to the in-situ lamina stress-strain behavior. A unidirectional ply subjected to transverse tensile stress has a low resistance to crack propagation in a direction perpendicular to the applied load. As a result, an initial flaw can propagate indefinitely and cause failure. When this same ply is located in a laminate, the effect of the initial crack in the ply is suppressed by transference of stress to adjacent layers through interlaminar stresses. There exists the possibility that, within a laminate, transverse tension behavior might show the effect of non-linear behavior due to an accumulation of cracks parallel to the fibers as a result of the ply transverse stresses. There is no evidence that this occurred in the present tests. It should also be noted that the shear stress-strain curves were obtained from ±45° tensile coupons in which there is the opportunity for transverse cracks to accumulate, demonstrating the effect discussed above. Whether or not this was the cause of the non-linear shear stress-strain behavior cannot be determined from the experimental data obtained herein.

In any event, since most practical laminates are constructed with at least three fiber directions, shear strains induced within individual plies due to both load and thermal stresses tend to

be small. Because of this, and since the material did not exhibit non-linearity transverse to the fibers in the basic material, the effect of non-linear stress-strain curves upon the observed thermoelastic behavior of the laminate studied herein was minimal. This effect may be regarded as a minor effect for practical laminates of this carbon-fiber/polyimide composite.

A related phenomenon was observed to have a significant effect; namely, the influence of temperature dependent properties upon the observed thermomechanical behavior. Prediction of thermal expansion characteristics and solution of any thermal stress problem for a composite laminate having temperature-dependent properties requires knowledge of the laminate stress free temperature. Solution of the thermoelastic, temperature-dependent problem requires definition of the stress free temperature state, knowledge of the mechanical properties at the final temperature and definition of the total free thermal expansions of the ply material when subjected to a temperature change from stress free temperature to final temperature. With this information the stresses and strains at any final temperature can be determined. The calculated laminate thermal expansion curves shown in figures 5-7, based on two different stress free temperatures, show that there is a substantial percentage difference between the two sets of calculations. Although laminate thermal expansion coefficients for this case are small, such behavior can be of significance in the design of dimensionally stable composite structures.

The second major area of concern was the possibility of time dependent behavior of these high temperature composite materials. Polymers subjected to stresses and strains at temperature levels approaching the glass transition temperature can be expected to show viscoelastic or similar time dependent response characteristics. As a result of this, a series of calculations were carried out to quantify the nature of this effect. In the absence of direct experimental data on the viscoelastic characteristics of

the particular carbon fiber/polyimide matrix composite under consideration, representative data were taken from the literature in these calculations.

The first problem studied was the stress relaxation in laminates. The problem considered was the rate of relaxation of the stresses induced by the curing process; such residual stresses existing in a laminate which is not subjected to any load and is held at a constant temperature. The laminate treated was a quasi-isotropic laminate. The results are identical for a 0/90 or ±45° laminate. A closed form solution was found for the case where the material properties can be adequately modeled by Maxwell behavior. In this case, the relaxation time for the laminate was found to be slightly larger than the relaxation time for the laminae material. However, the difference between the two is small.

In order to assess the significance of material viscoelasticity in the response of a practical structure, the same laminate was analyzed for temperature cycles from -157°C to +316°C over a 24 hour period. This was representative of a composite space structure in orbit. The results indicated that the total amplitude of the change in strain during a single temperature excursion from minimum to maximum remained essentially constant while the mean value shifted. The laminate approached the case of a steady state cycle wherein the maximum strain was zero, and the minimum strain was negative. The significance of this is associated with the question of dimensional stability: the potential problem being that the actual range of dimensional change during service can differ significantly from the dimensional changes measured during initial cycling tests of the "as manufactured" structure.

Finally, one additional concern should be recognized; stress relaxation has the effect of changing the stress free temperature of a laminate. Changes in stress free temperature have been shown

to change the subsequent response characteristics of a laminate subjected to a temperature change. Hence, additional uncertainty exists with regard to dimensional stability.

CONCLUSIONS

An evaluation has been conducted of the effects upon the behavior of carbon-fiber/polyimide-matrix composite laminates of material non-linearity due to either: high lamina stresses, or time-dependent lamina material behavior.

Based on the results of the present study, it appears that non-linearities due either to stress or time dependent effects do not appear to be of major practical importance for conventional high temperature composite structures. However, the effects of time dependent characteristics and temperature dependent properties can be of significance in understanding the behavior of dimensionally stable structures designed for long lifetimes.

REFERENCES

1. Hashin, Z., Rosen, B.W., and Pipes, R.B., "Non-linear Effects on Composite Thermal Expansion," NASA CR-3088, February 1979.

2. Hashin, Z., Bagchi, D., and Rosen, B.W., "Non-linear Behavior of Fiber Composite Laminates," NASA CR-2313, April 1974.

3. Kibler, K.G., et al., "Time-Dependent Environmental Behavior of Graphite-Epoxy Composites," Quarterly Progress Report No. 8, (June 1 - August 31, 1981), General Dynamics, Project No. 2419/03, Air Force Materials Laboratory, September 17, 1979.

4. Kibler, J.J., Derby, E.A., Chatterjee, S.N., and Oscarson, J., "Structural Assessment of 3-D Carbon-Carbon Cylinders During Processing," AFML-TR-78-75, April 1978.

5. Christensen, R.M., "Theory of Viscoelasticity, An Introduction," Academic Press, NY, 1971, pp. 92-104, 218-221.

6. Halpin, J.C., "Introduction to Viscoelasticity," Composite Materials Workshop, Tsai, S.W., Halpin, J.C., and Pagano, N.J., editors, Technomic Publishing Company, 1968.

7. Yeow, Y.T., Morris, D.H., and Brinson, H.F., "Time Temperature Behavior of a Unidirectional Graphite/Epoxy Composite," Composite Materials: Testing and Design (5th Conference), ASTM STP 674, Tsai, S.W., ed., American Society for Testing and Materials, 1979, pp. 263-281.

8. Farley, G.F., "Effects of Static Tensile Load on the Thermal Expansion of Gr/Pi Composite Material," NASA TP-1867, June 1981.

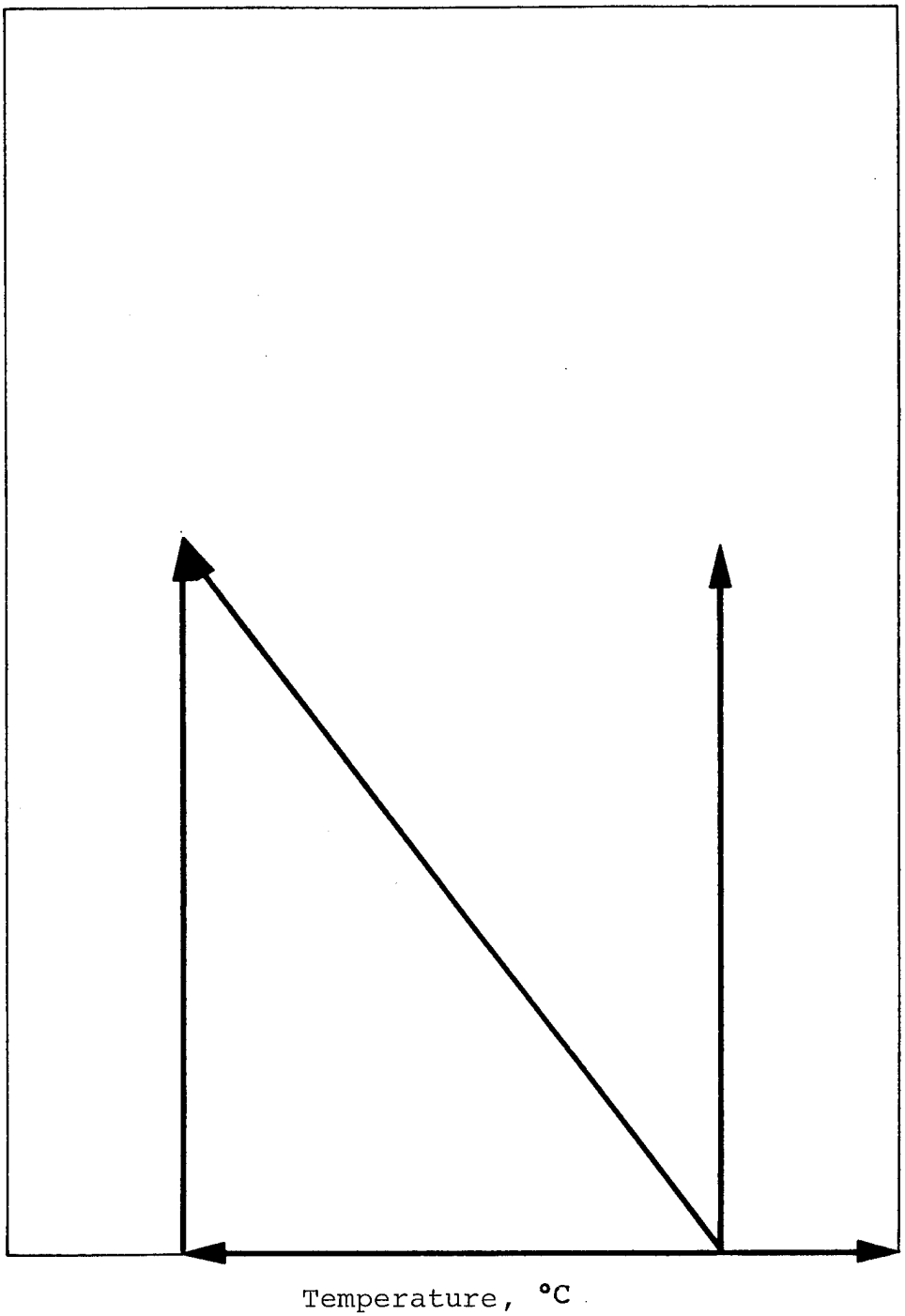

Figure 1. Load Temperature Space - Load Paths

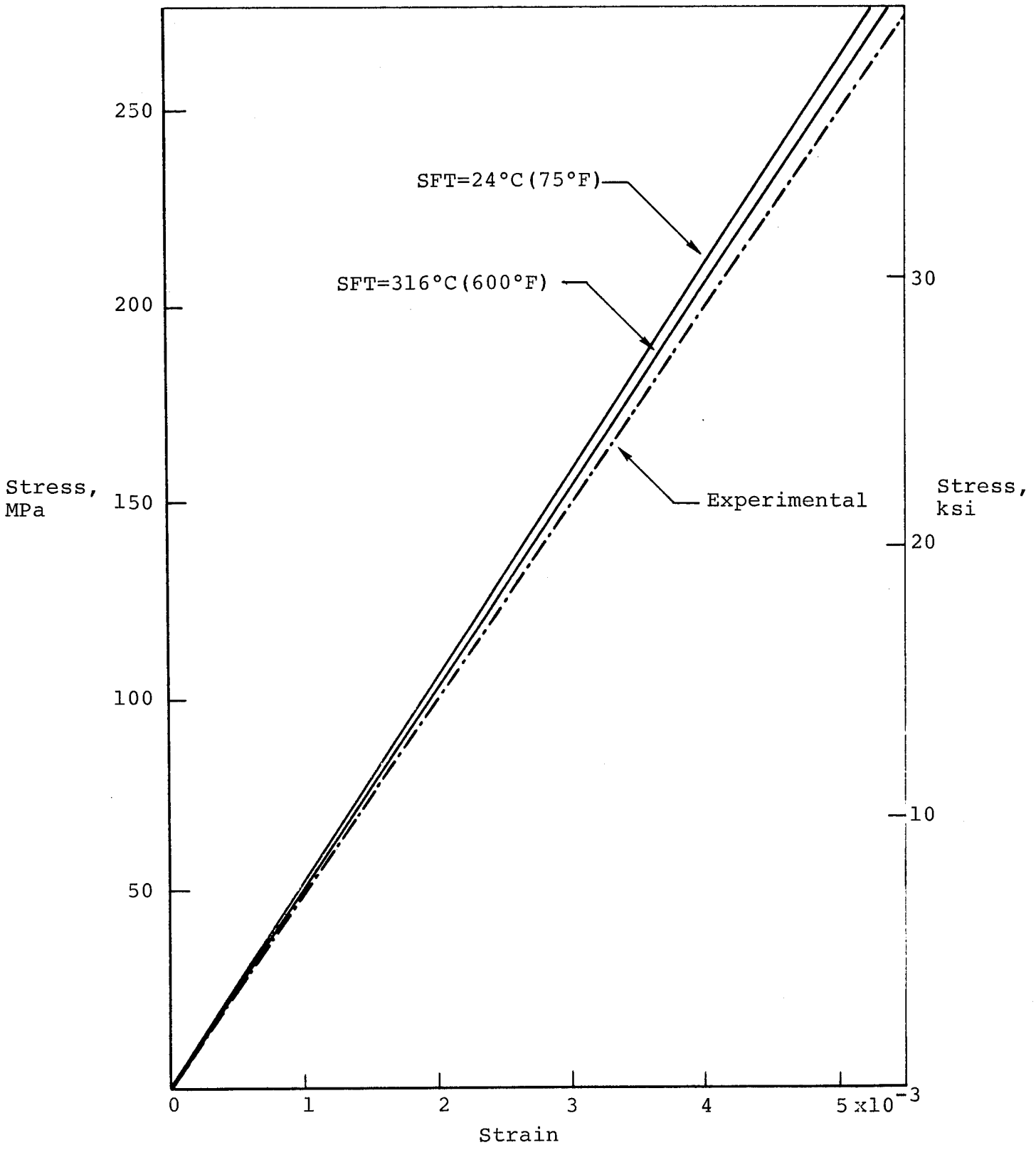

Figure 2. Stress-Strain Response of a Quasi-Isotropic $[0/\pm45/90]_s$ Laminate at 24°C (75°F)

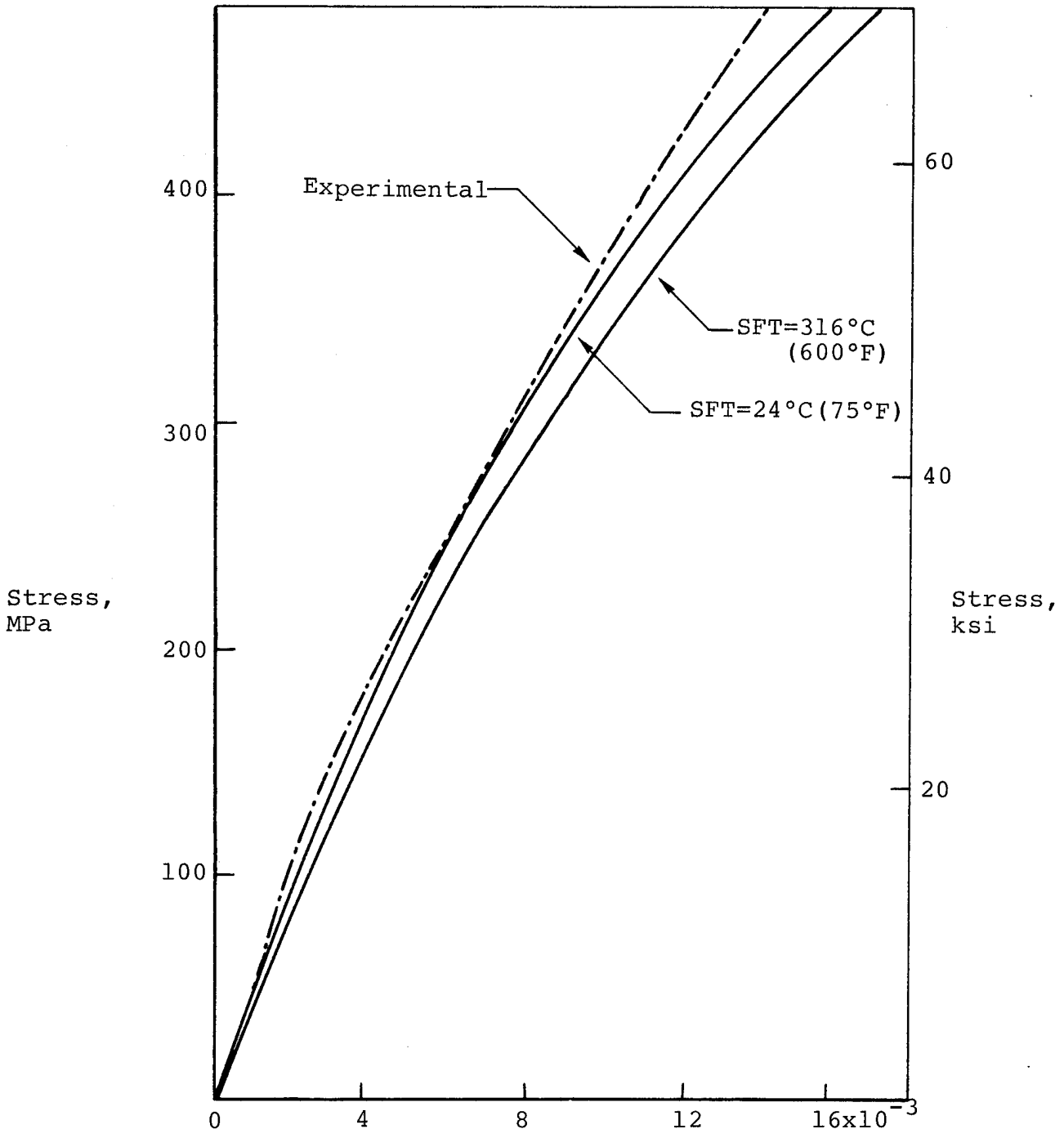

Figure 3. Stress-Strain Response of a $[\pm 30]_s$ Laminate at 24°C (75°F)

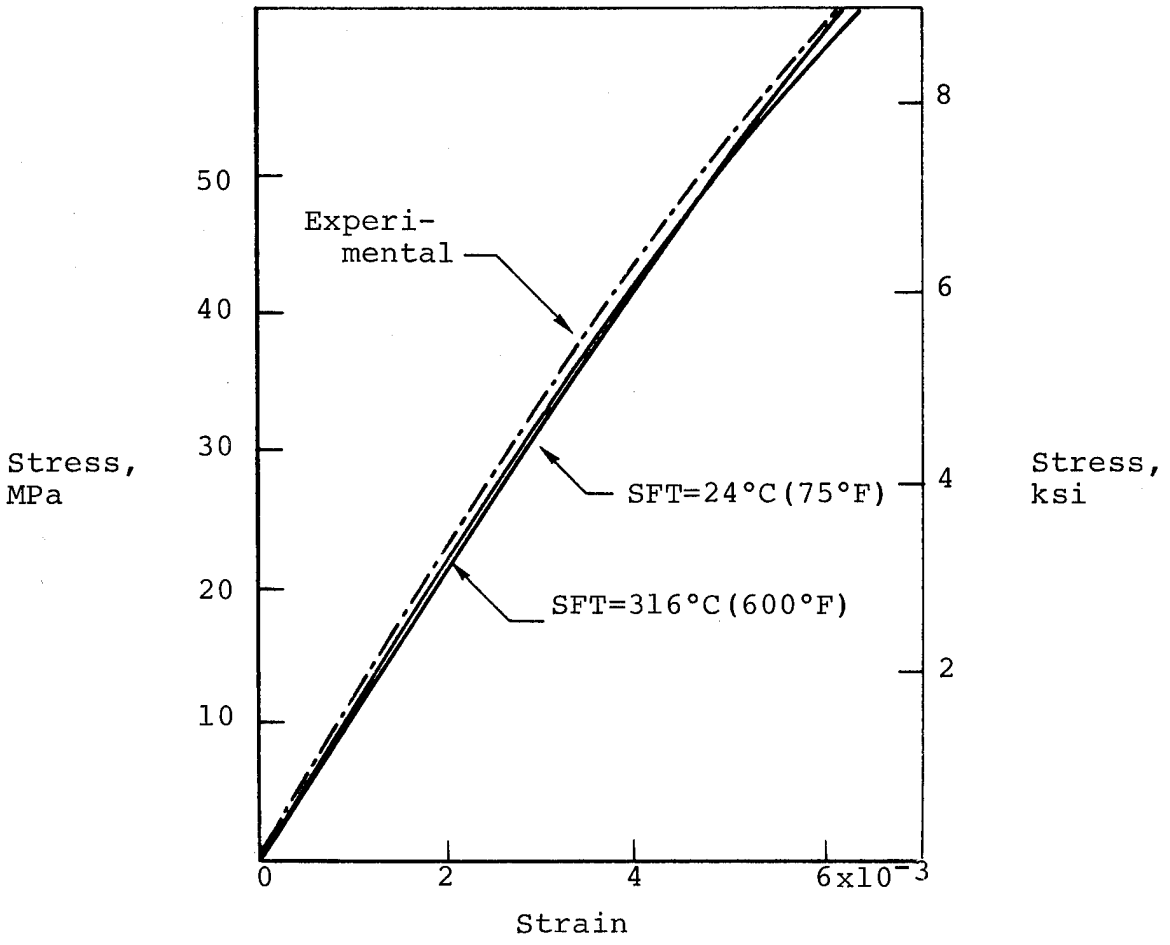

Figure 4. Stress-Strain Response of a $[\pm 60]_s$ Laminate at 24°C (75°F)

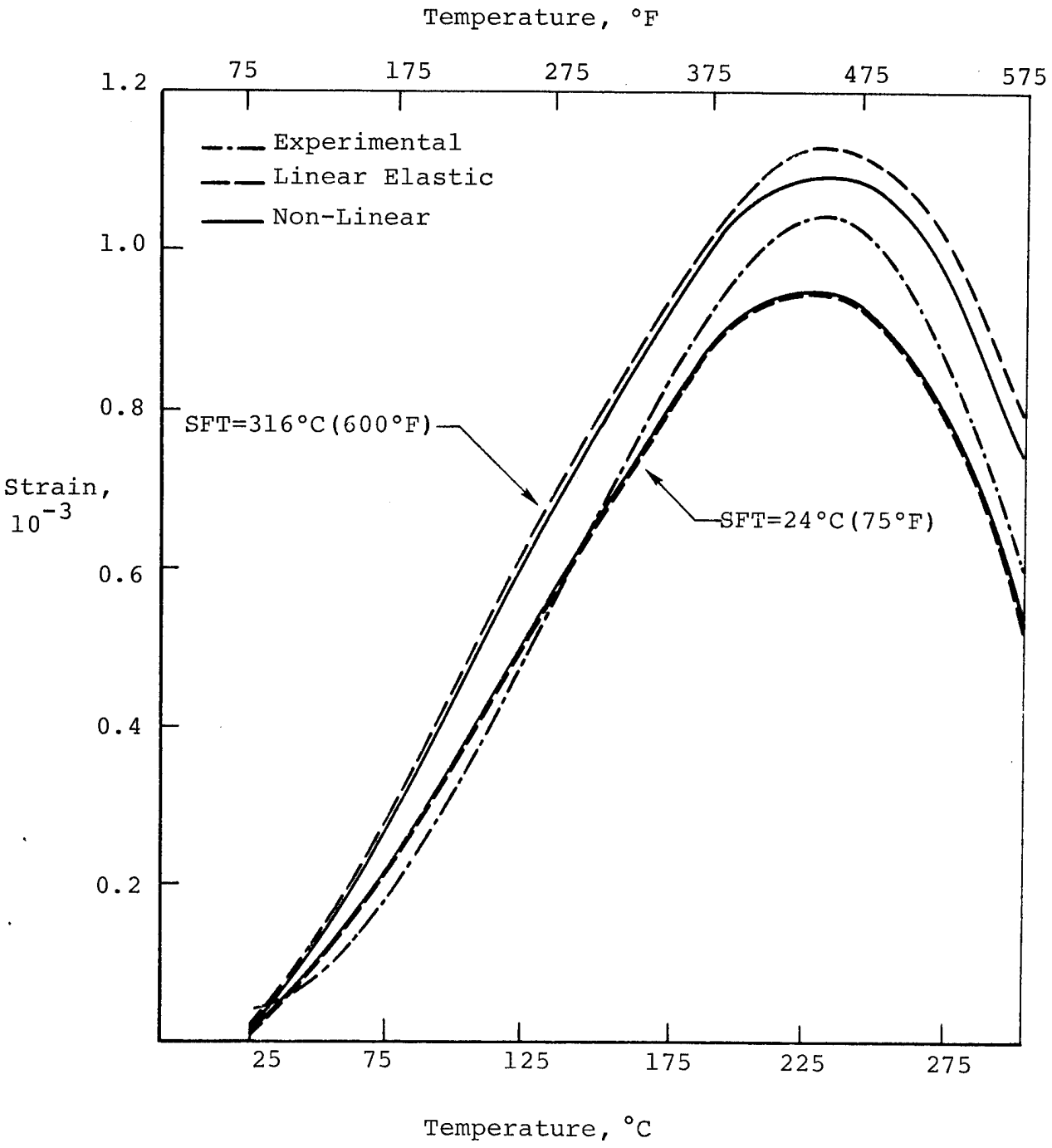

Figure 5. Free Thermal Expansion of a $[0/90]_s$ Laminate

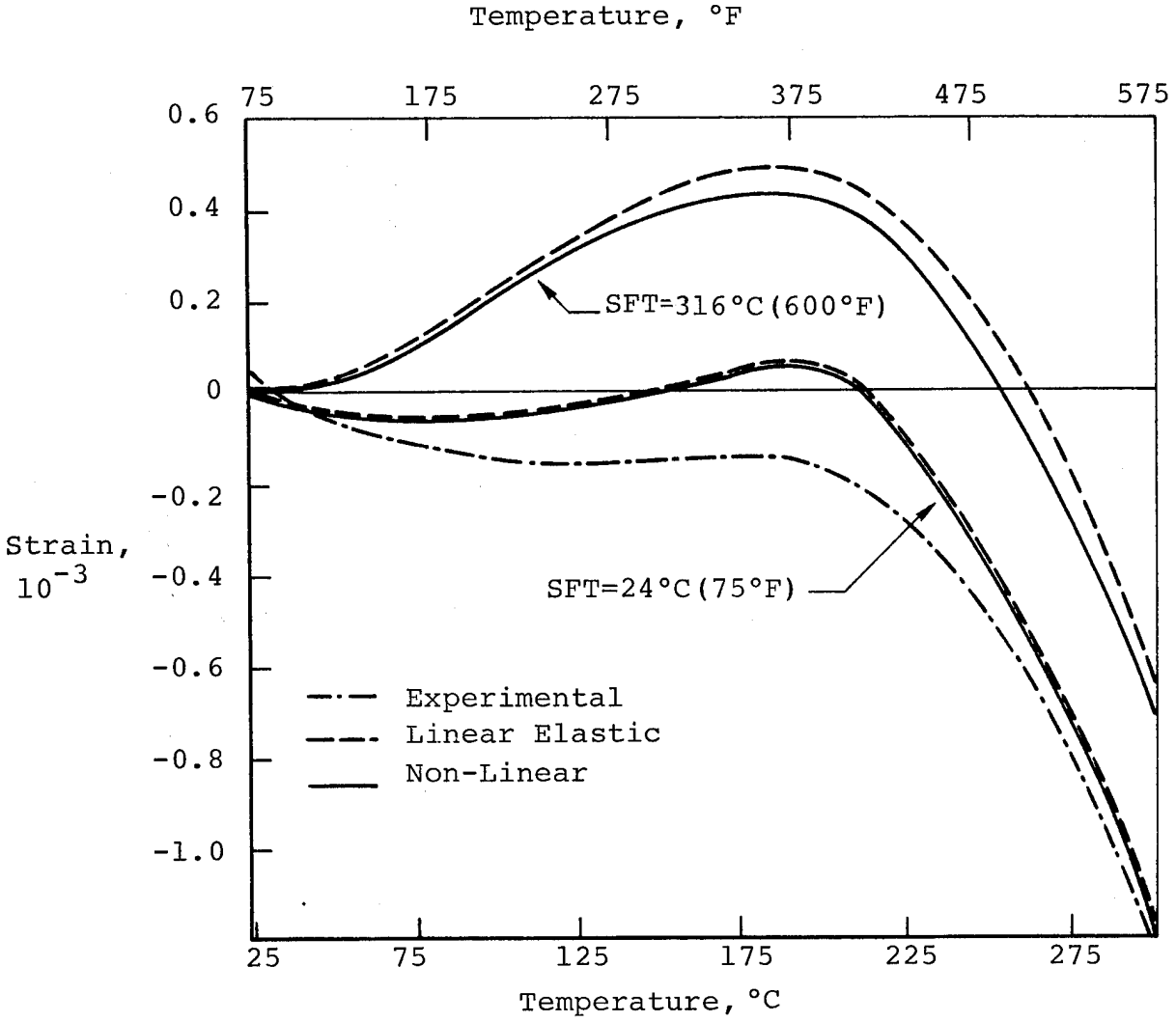

Figure 6. Free Thermal Expansion of a $[\pm 30]_s$ Laminate

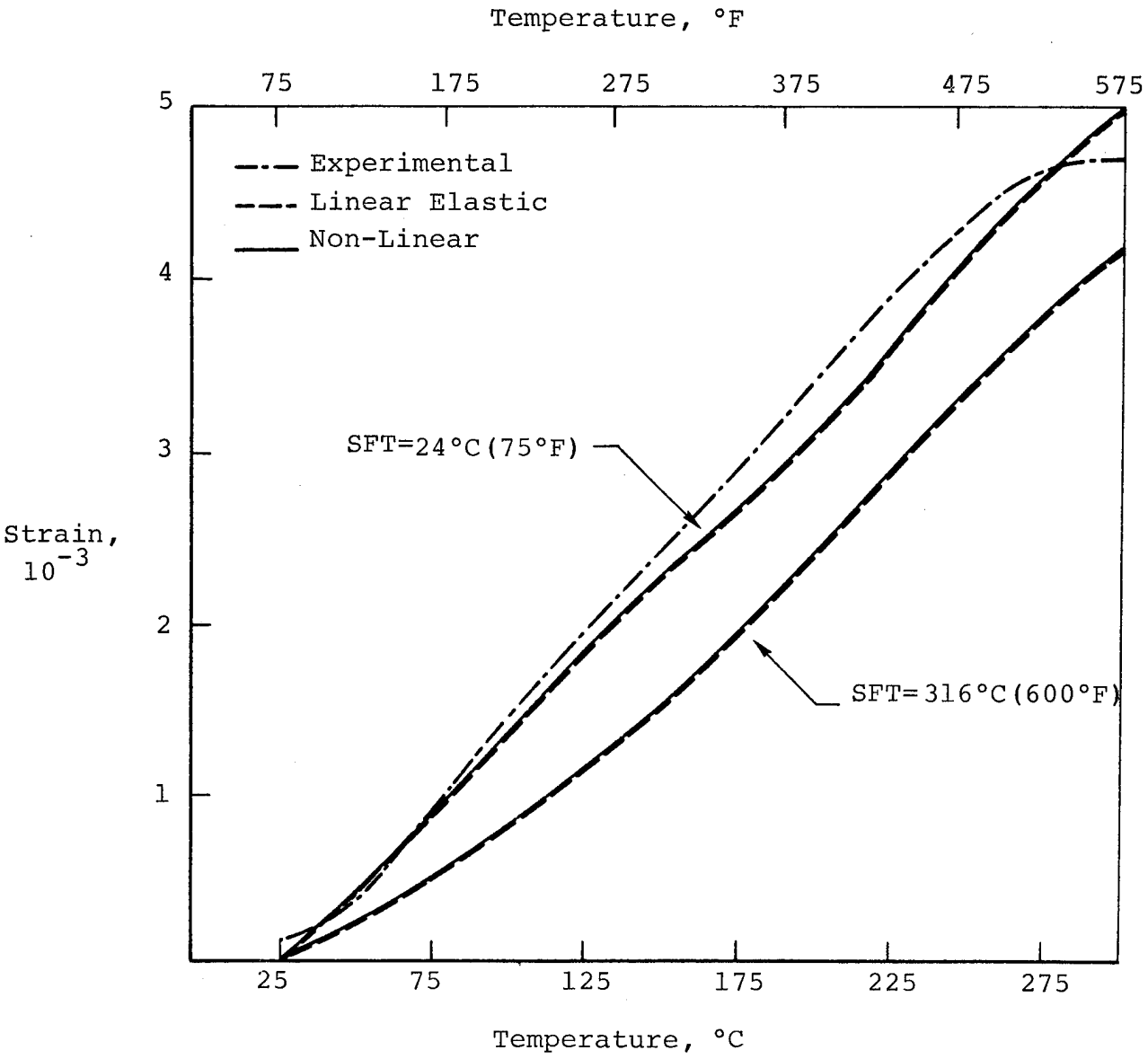

Figure 7. Free Thermal Expansion of a $[\pm 60]_s$ Laminate

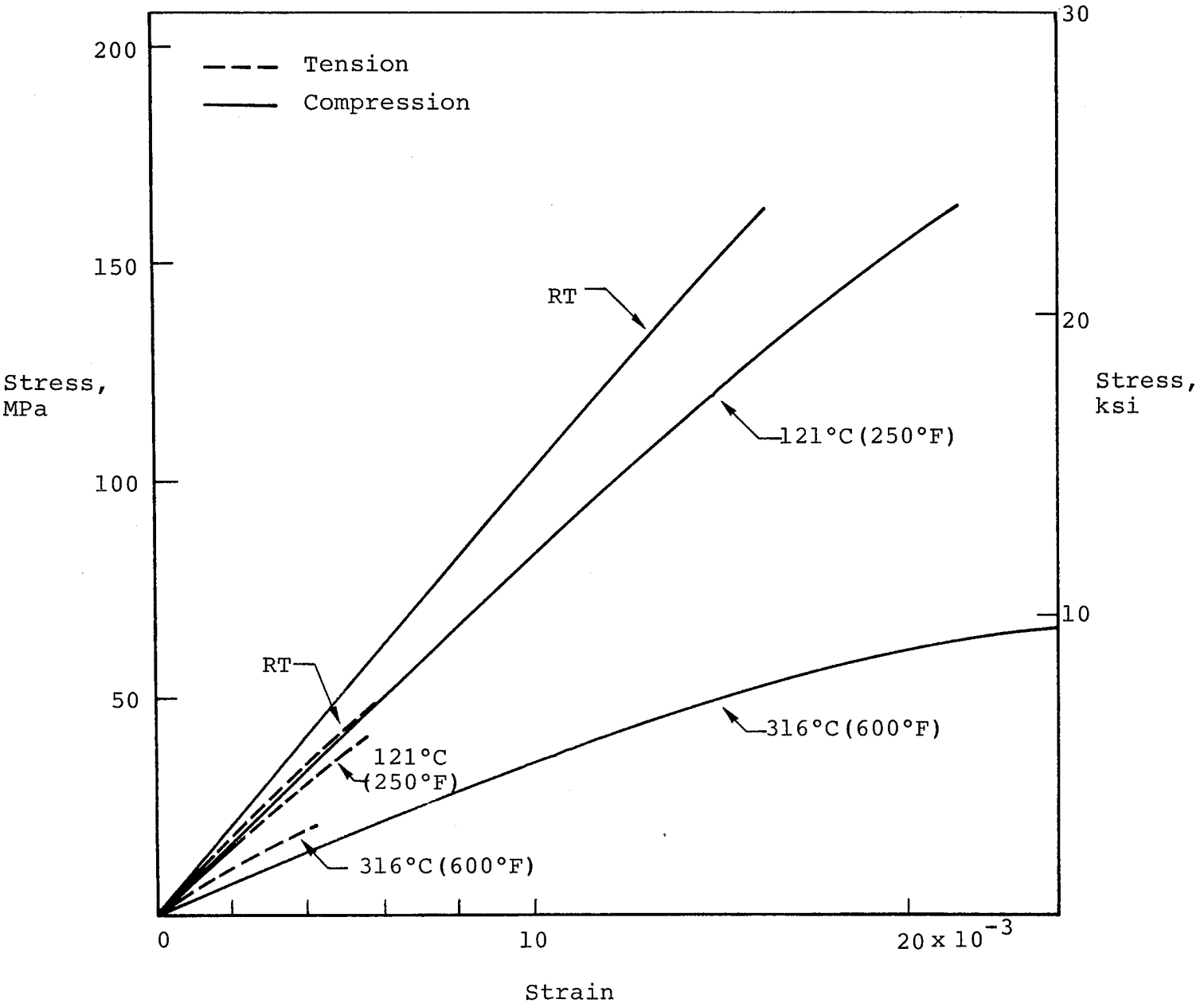

Figure 8. Transverse Stress-Strain Response of Graphite/Polyimide

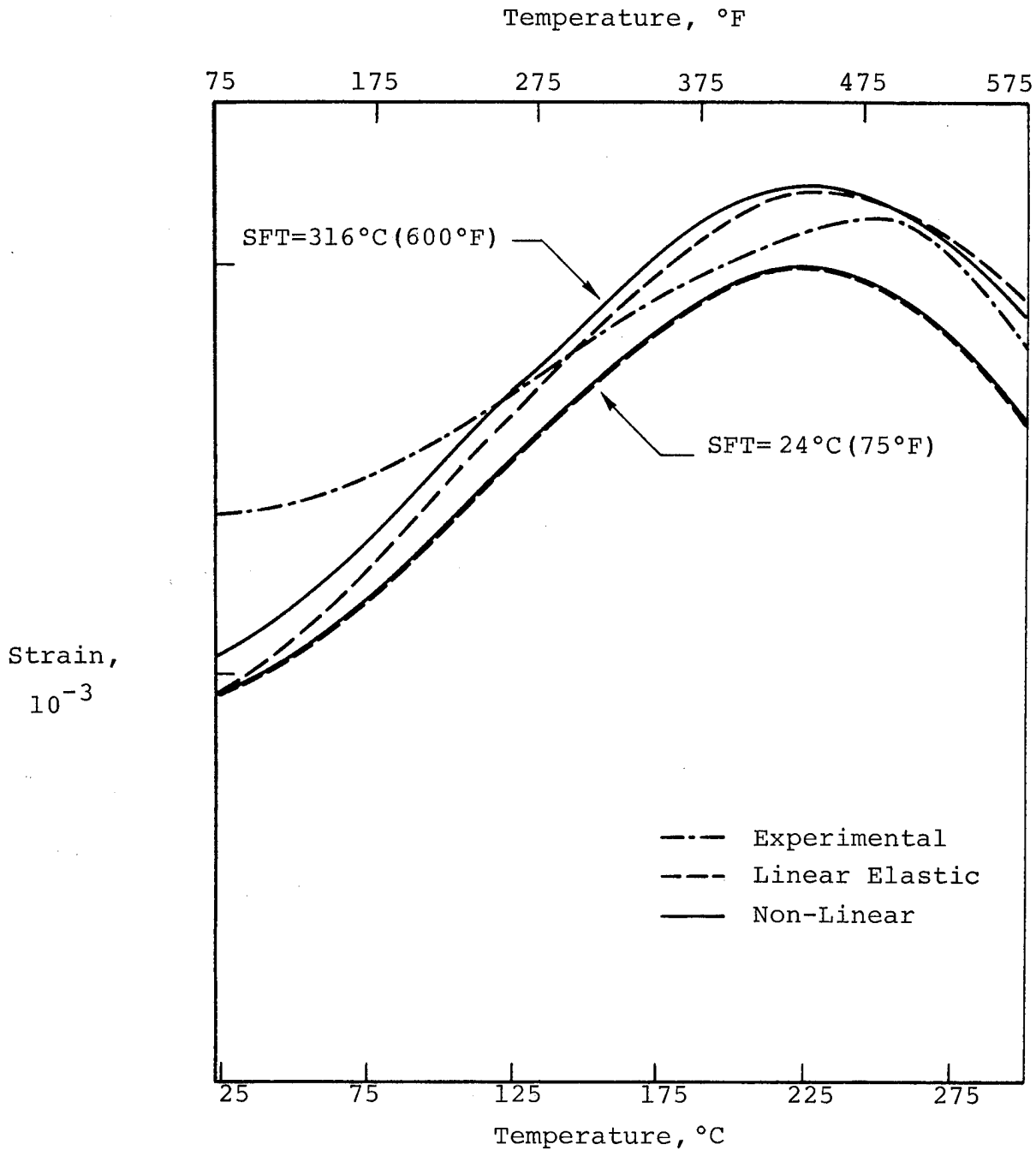

Figure 9. Thermal Expansion of a $[0/90]_s$ Laminate with a Constant Axial Load of 290 MPa (42 ksi)

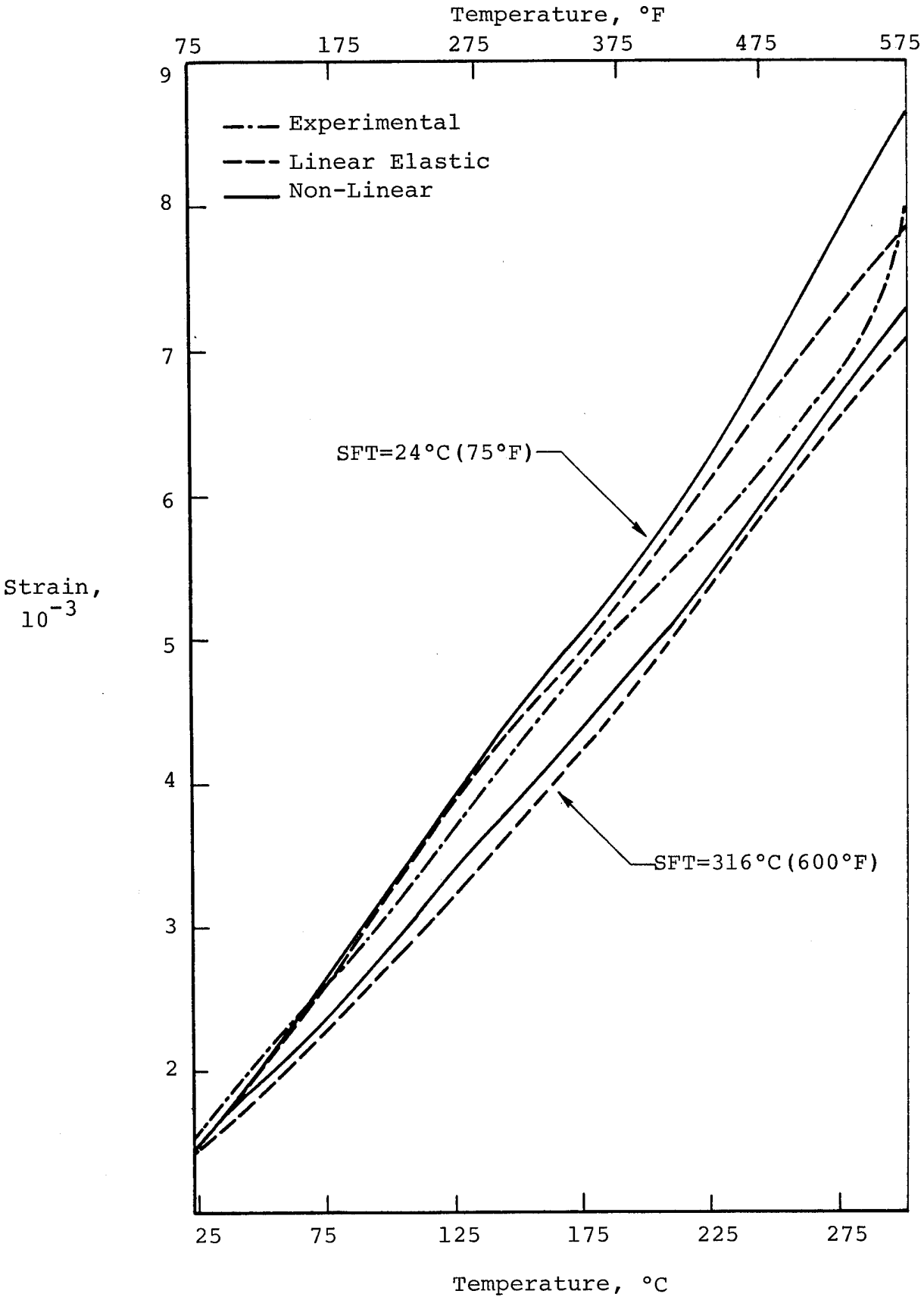

Figure 10. Thermal Expansion of a $[\pm 60]_S$ Laminate with a Constant Axial Load of 16 MPa (2.34 ksi)

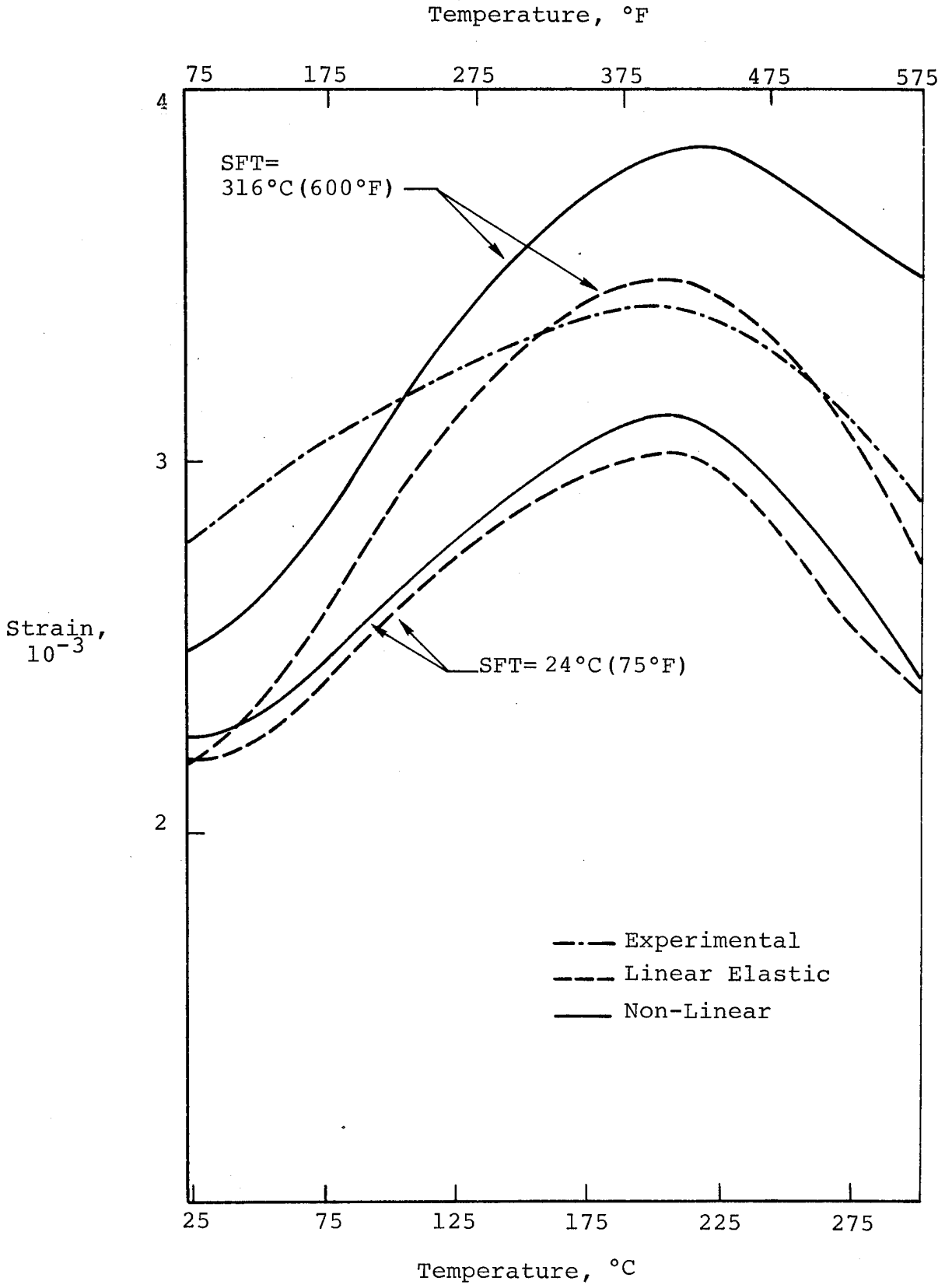

Figure 11. Thermal Expansion of a $[\pm 30]_S$ Laminate with a Constant Axial Load of 105 MPa (15.24 ksi)

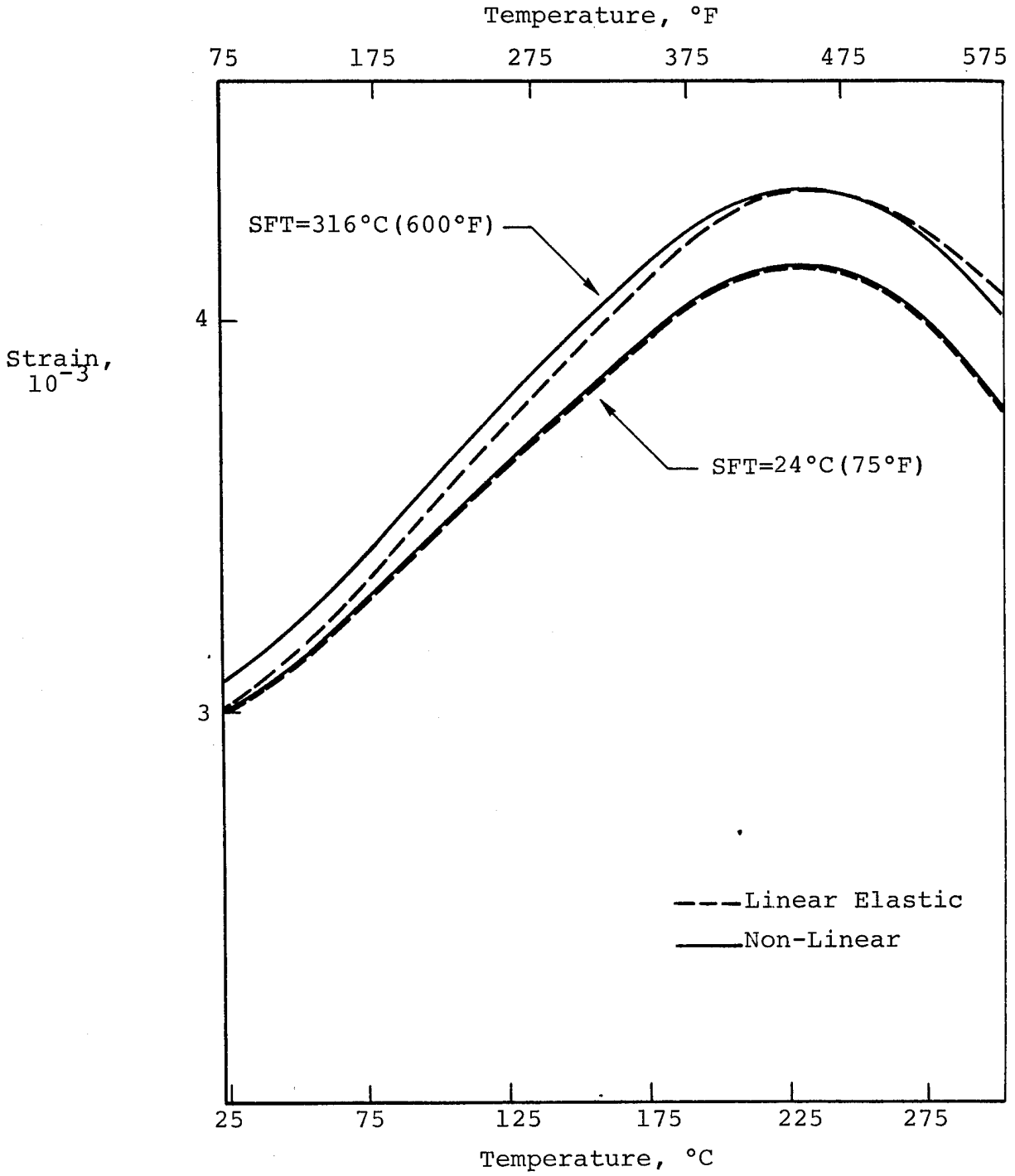

Figure 12. Thermal Expansion of a $[0/90/\pm45]_s$ Laminate with a Constant Axial Load of 159 MPa (29 ksi)

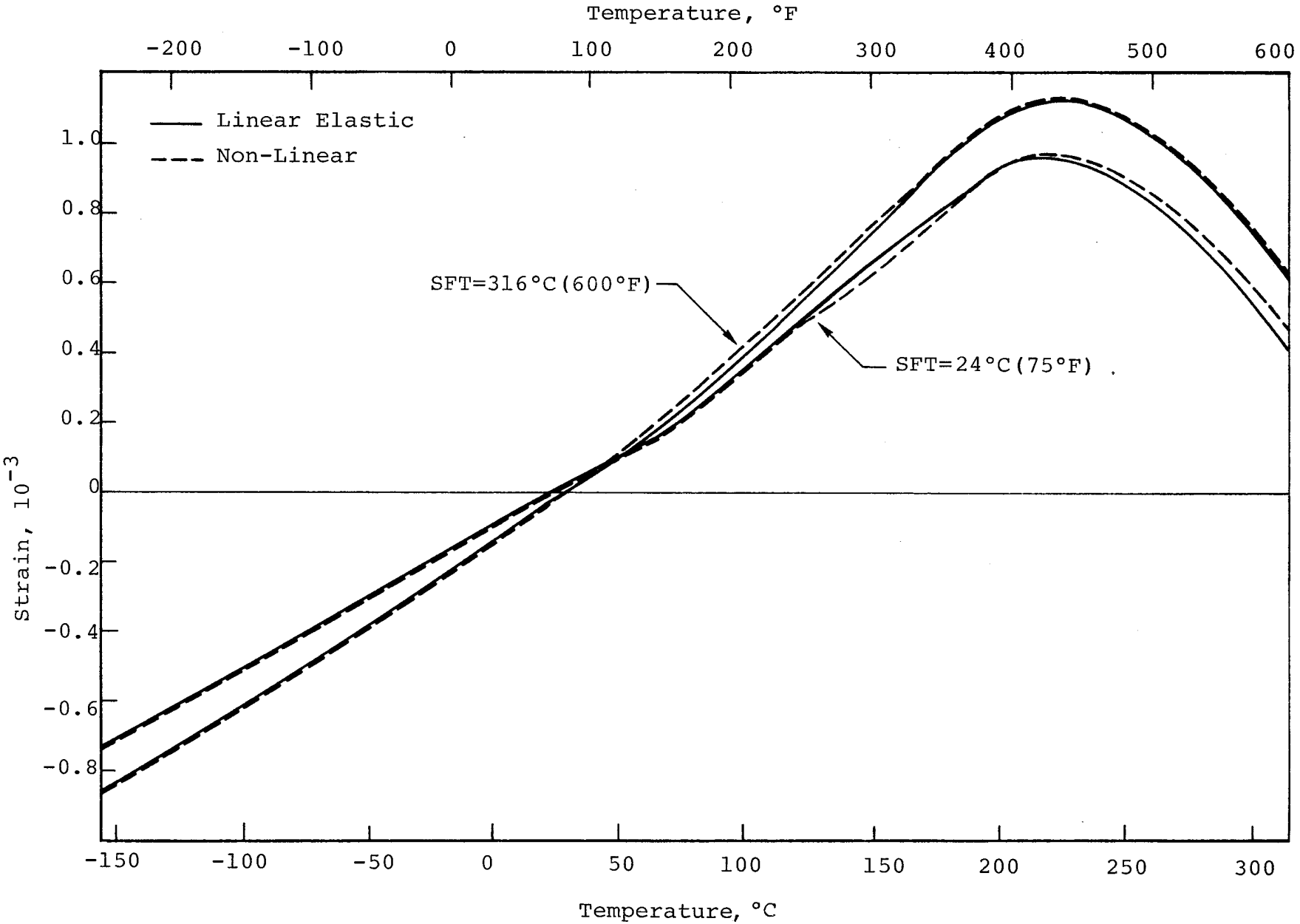

Figure 13. Thermal Expansion of a $[\pm 45]_S$ Laminate with a Constant Axial Load of 290 MPa (42 ksi)

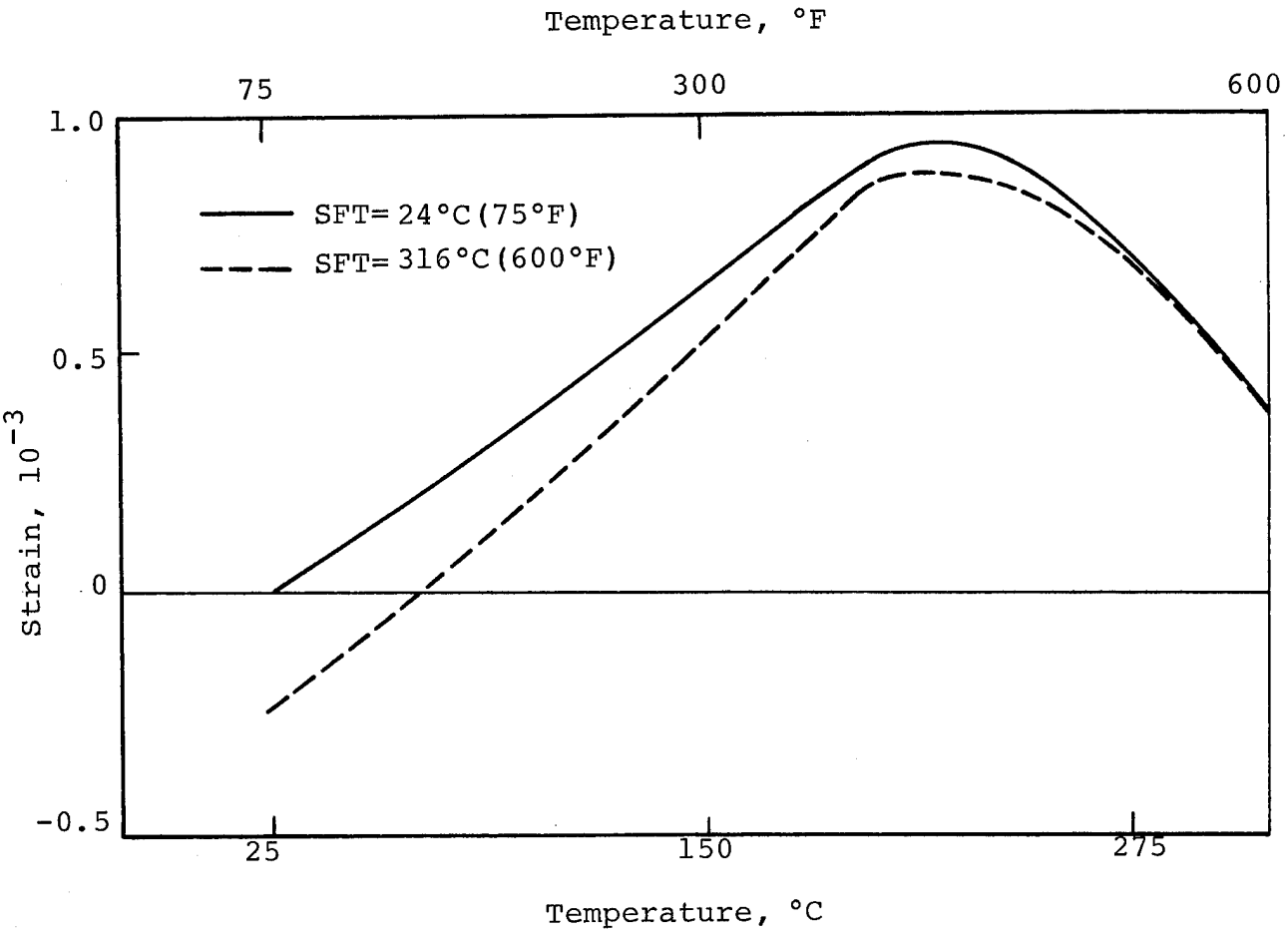

Figure 14. Thermal Cycling of a $[\pm 45]_s$ Laminate

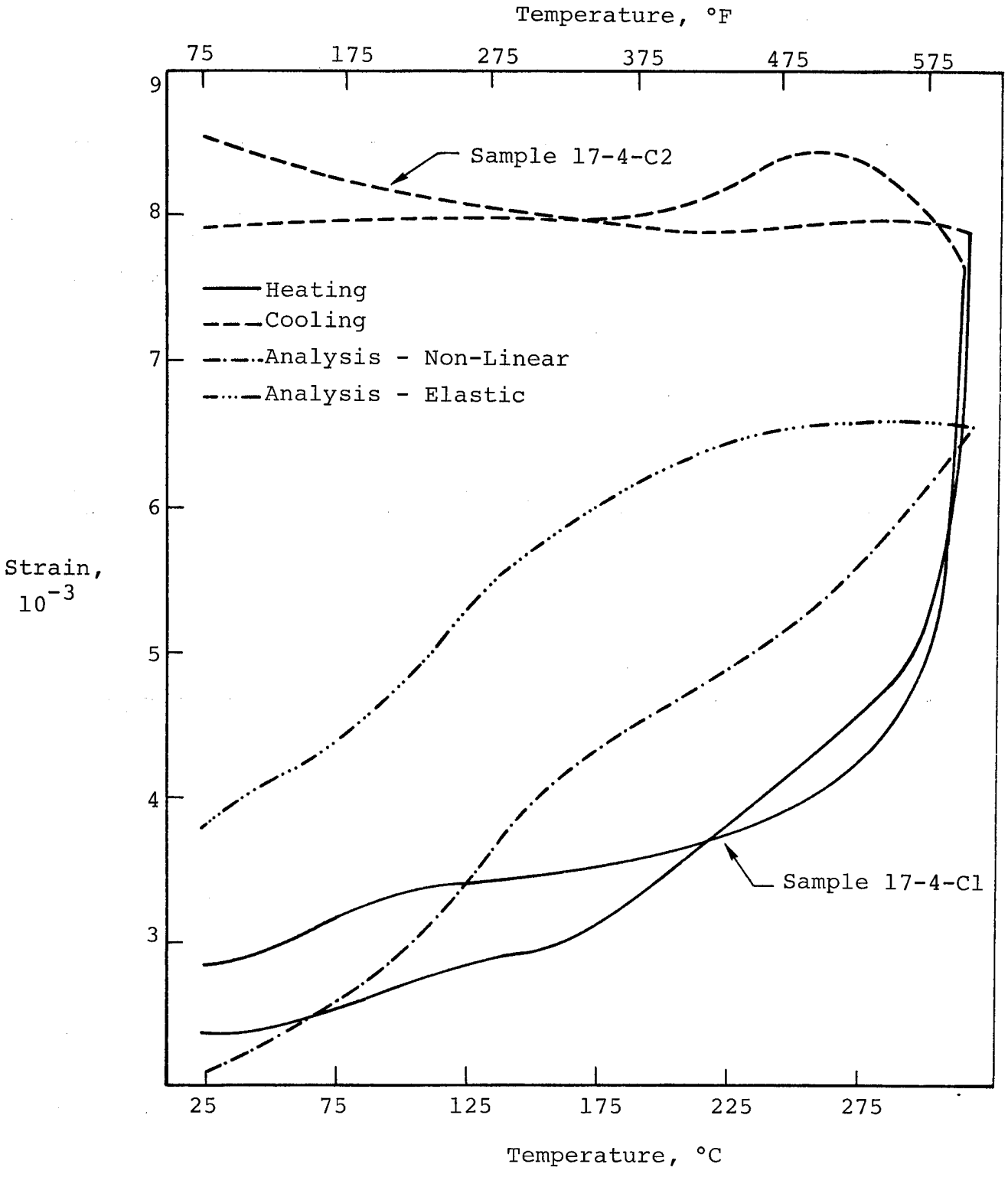

Figure 15. Thermal Cycling of a $[\pm 45]_S$ Laminate Under a Constant Axial Load of 34 MPa (5 ksi)

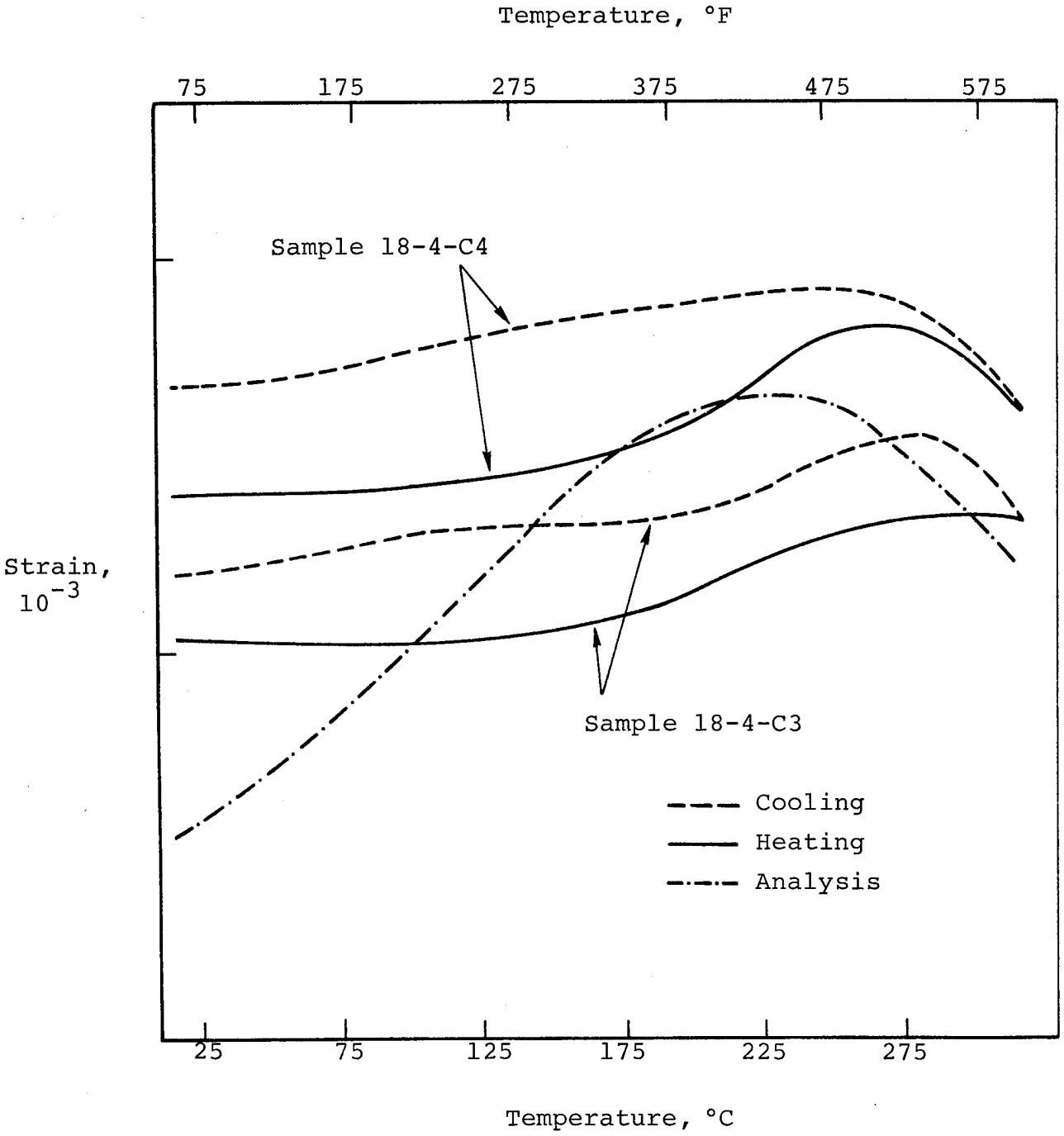

Figure 16. Thermal Cycling of a $[0/\pm45/90]_s$ Laminate Under a Constant Axial Load of 138 MPa (20 ksi)

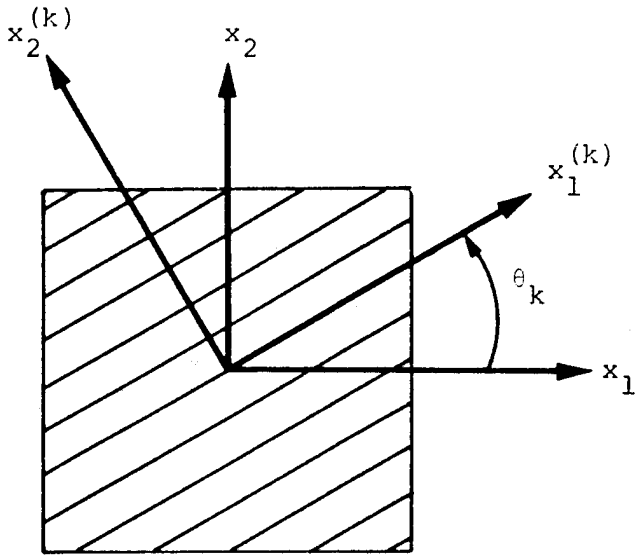

Figure 17. Laminate Geometry

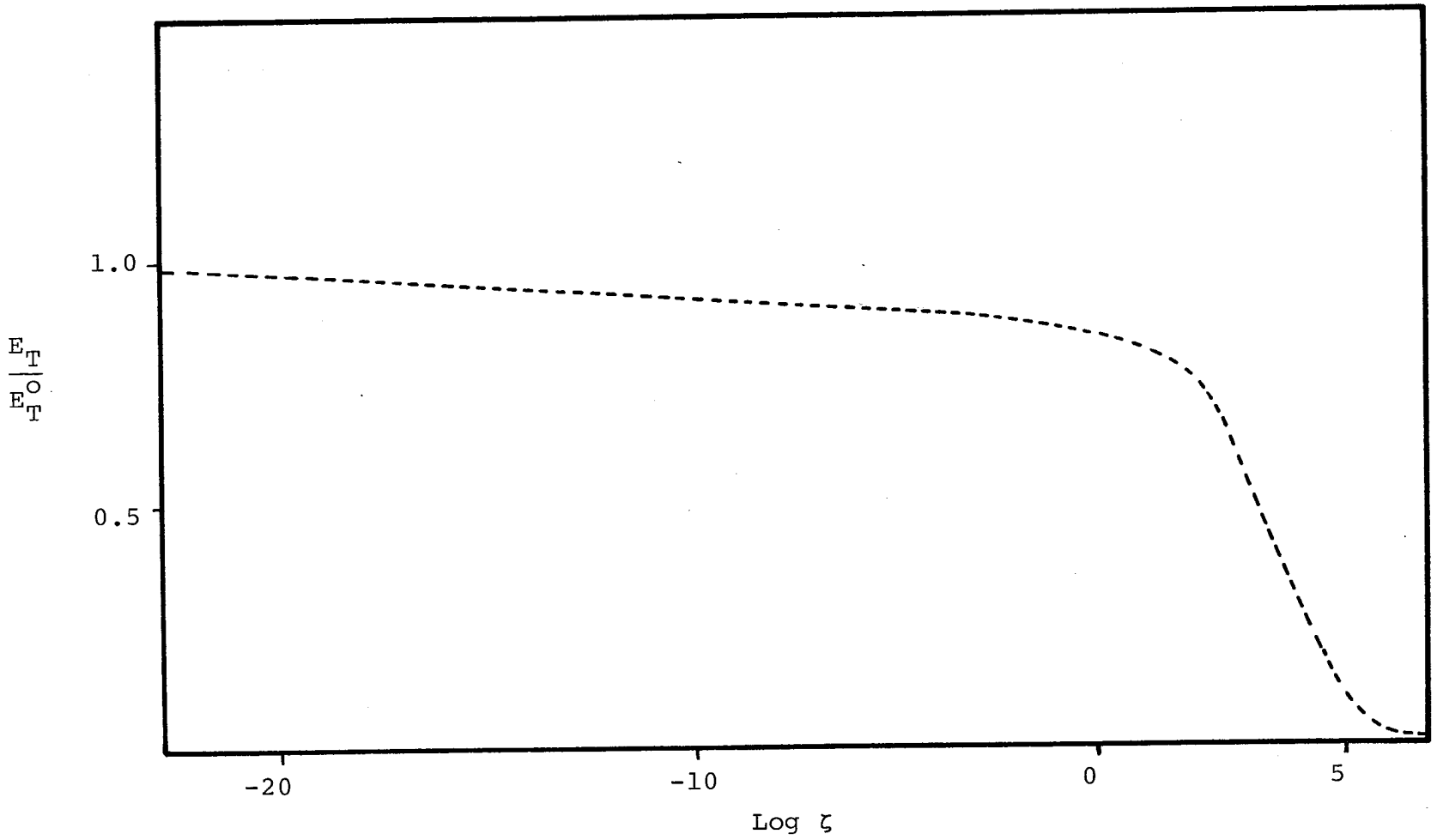

Figure 18. Relaxation Modulus Master Curve for Graphite/Epoxy, Reference Temperature 177°C (350°F)

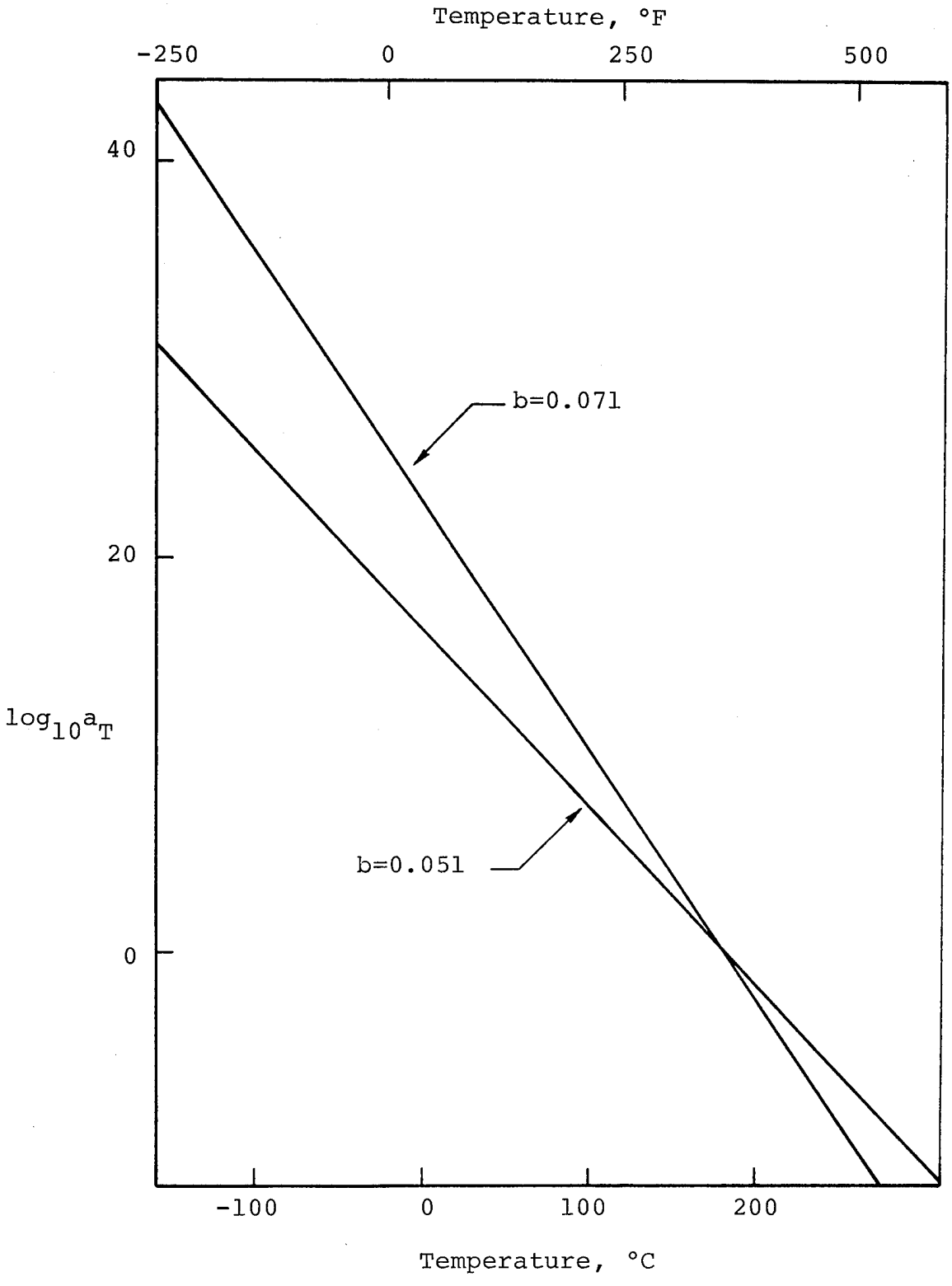

Figure 19. Time-Temperature Shift Factor Curve for Graphite/Epoxy

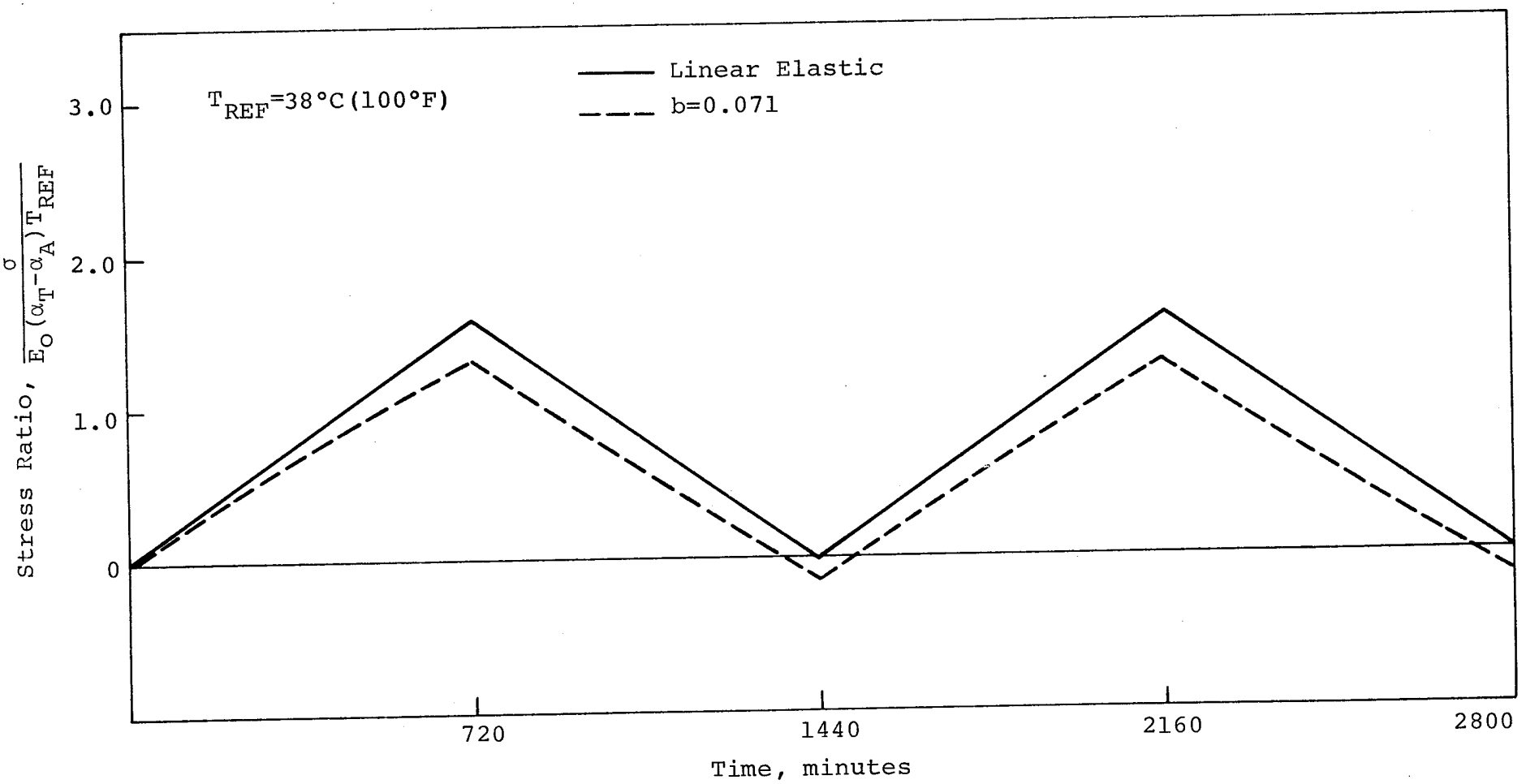

Figure 20. Stress Response of a $[0/90]_s$ Laminate for Cycling Between -18°C and 177°C (0°F and 350°F)

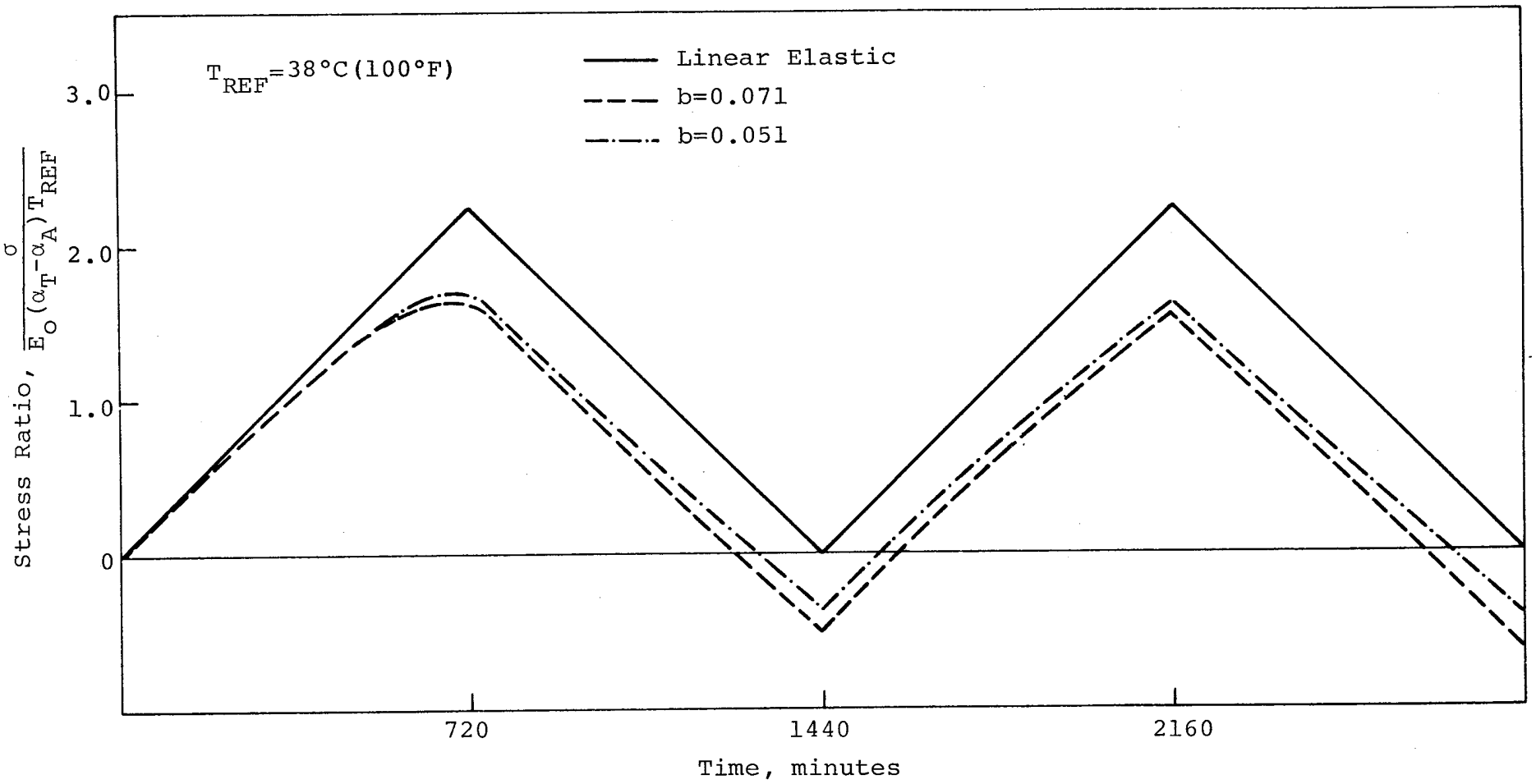

Figure 21. Stress Response of a $[0/90]_s$ Laminate for Cycling Between -73°C and 204°C (-100°F and 400°F)

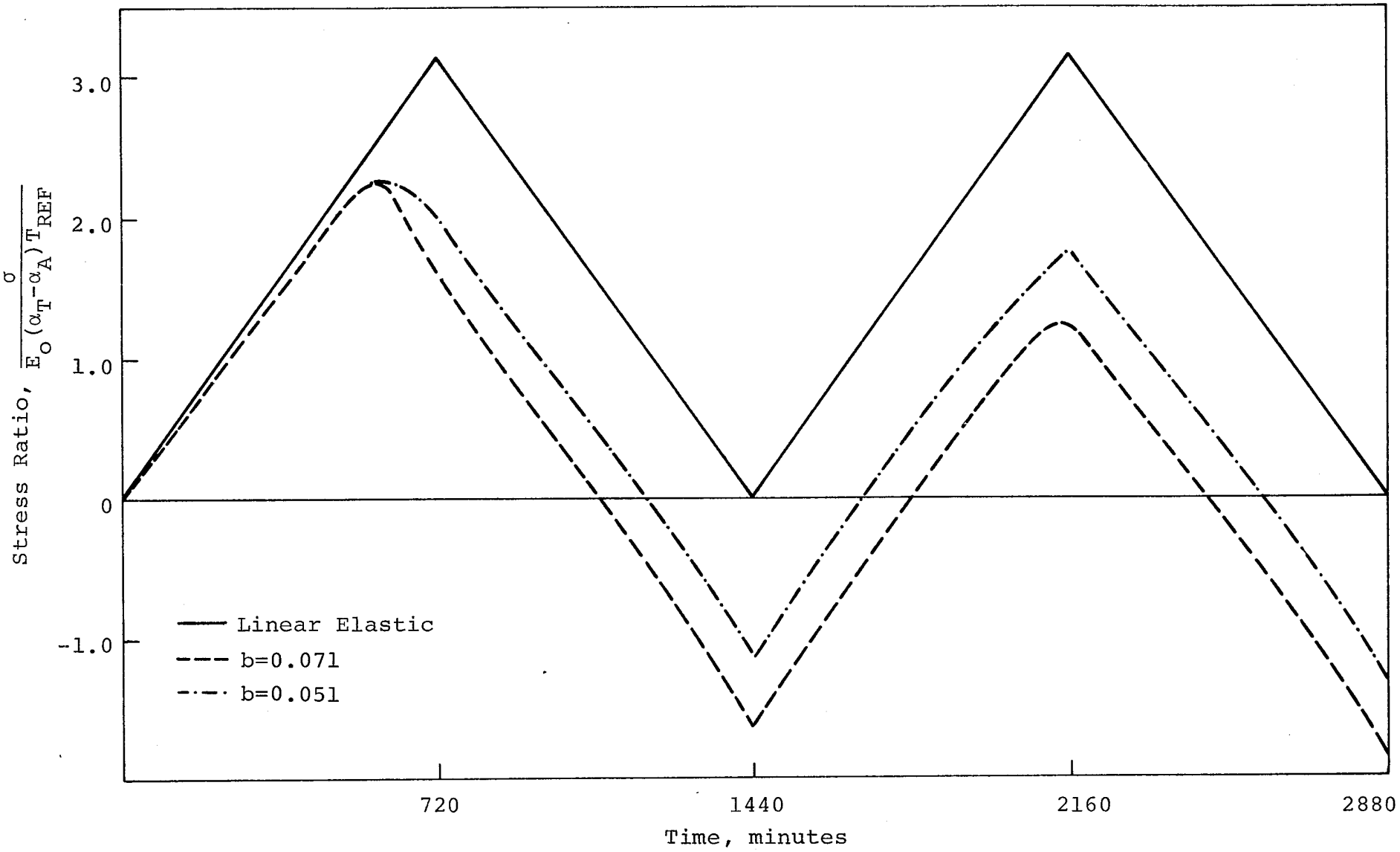

Figure 22. Stress Response of a $[0/90]_s$ Laminate for Cycling Between -157°C and 232°C (-250°F and 450°F)

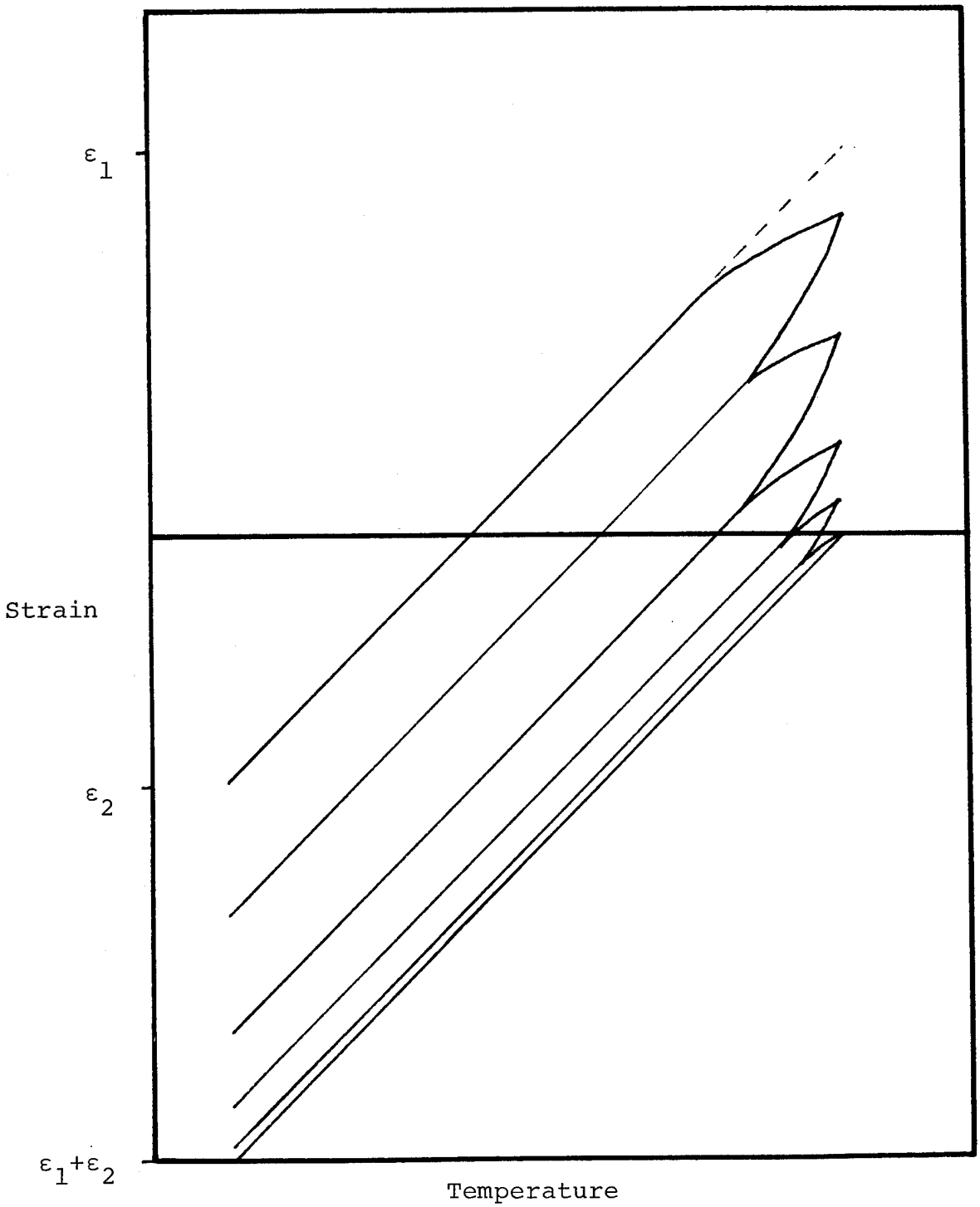

Figure 23. Strain Response to Thermal Cycling

APPENDIX A
NON-LINEAR THERMOELASTIC LAMINATE ANALYSIS

TENOL FORMULATION AND PROGRAM DESCRIPTION

Introduction

The TENOL program codifies a thermoelastic, non-linear, plane stress laminate analysis wherein the temperature-dependent non-linear behavior of the laminae under in-plane shear and transverse stresses are taken into account. Both the underlying analytical development and the computer program are sufficiently general to enable the user to study the non-linear behavior of a symmetric laminate subject to any combination of temperature, in-plane shear and biaxial loadings. Contained in this document are a detailed description of the input required to use the program and a brief outline of the theoretical development on which the program is based. The reader is referred to references A-1 and A-2 for the complete analytical development. Portions of these references are reproduced herein.

In most unidirectional fiber-reinforced materials, the transverse extensional and particularly the in-plane shear behavior are non-linear. This non-linearity increases with temperature and is very prominent at elevated temperatures. The program TENOL allows for non-linear representation of the stress-strain behavior by Ramberg-Osgood approximations. The introduction of these non-linear constitutive relationships into a lamination theory analysis leads to a set of non-linear equations with the laminar stresses as unknowns. The program then solves this set of equations utilizing the generalized Newton-Raphson iterative procedure, yielding the laminae stresses and strains corresponding to the applied boundary conditions.

The theoretical development for this non-linear laminate analysis incorporates a thermoelastic total deformation theory with the Ramberg-Osgood constitutive relations to formulate the governing equations at the final temperature of the laminate. At a given

temperature, the compliance tensor is assumed to be the sum of two tensors; the components of one are the usual components associated with linear, orthotropic, plane stress elasticity theory, while the second tensor contains the non-linear elements. By assuming a quadratic interaction of the stress components, and requiring the constitutive relationship to reduce to the relationships for the uniaxial stress cases of in-plane shear and transverse extension, the elements of the non-linear compliance tensor are explicityly determined.

Having the non-linear laminae constitutive relations, the usual methods of laminate theory are then utilized to obtain the governing non-linear equations for the laminate. As in linear laminate theory, the strains of the individual laminae are first rotated to a common set of laminate axes, and the laminate compatibility relations requiring the corresponding strains of the individual laminae to be equal are then employed. In addition, equilibrium at the laminate boundaries is invoked. In this way, the required number of equations involving the unknown laminae stresses are formulated.

The program solution procedure for the set of non-linear equations involving the laminae stress components is a Newton-Raphson technique generalized to accommodate systems of equations. The starting point for the solution procedure is taken as the solution of the associated linear laminate problem, where the associated linear problem is obtained by ignoring all non-linear terms.

Incorporated into the program are three different failure criteria: maximum stress, maximum strain and a quadratic interaction criterion. All or any of these may be employed by the user.

Derivation of Governing Equations

In the usual plane-stress, linear, thermoelastic, laminate analysis, the laminae stress-strain relationships are first written with respect to the longitudinal and transverse fiber directions. These laminae relationships are then transformed to a

common set of laminate axes and the laminate constitutive relationships are then developed by enforcing strain compatability. In this non-linear laminate analysis an entirely analogous procedure is followed. The laminae non-linear, stress-strain relationships are first written for the N laminae with reference to their respective natural axes, and then transformed to a common set of laminate axes. Enforcement of compatibility between adjacent laminae as well as equilibrium at the laminate boundaries leads to the governing non-linear equations.

Let the strains be separable into linear, non-linear and free thermal parts:

$$\varepsilon_{11} = \varepsilon'_{11} + \varepsilon''_{11} + \alpha_{11}\Delta T$$

$$\varepsilon_{22} = \varepsilon'_{22} + \varepsilon''_{22} + \alpha_{22}\Delta T \qquad \text{(A-1)}$$

$$\varepsilon_{12} = \varepsilon'_{12} + \varepsilon''_{12}$$

where primes designate the linear parts and the double primes designate the non-linear parts, and the subscripts 1 and 2 refer to the longitudinal and transverse directions, respectively. The linear parts of the strain components are related to the stress components by the usual orthotropic, plane-stress, elasticity constitutive relationship:

$$\varepsilon'_{11} = \frac{1}{\varepsilon_{11}(T)}\,\sigma_{11} - \frac{\nu_{21}}{\varepsilon_{22}(T)}\,\sigma_{22}$$

$$\varepsilon'_{22} = -\frac{\nu_{12}}{\varepsilon_{1}(T)}\,\sigma_{11} + \frac{1}{\varepsilon_{22}(T)}\,\sigma_{22} \qquad \text{(A-2)}$$

$$\varepsilon'_{12} = \frac{1}{2G_{12}(T)}\,\sigma_{12}\,.$$

For the uniaxial stress states of transverse extension and in-plane shear, the non-linear parts of the strain components are related to the stress components by the relationships:

$$\varepsilon_{22}^{"} = \frac{\sigma_{22}}{\varepsilon_{22(T)}} \left(\frac{\sigma_{22}}{f_1}\right)^{n-1}$$

$$\varepsilon_{12}^{"} = \frac{\sigma_{12}}{2G_{12}} \left(\frac{\sigma_{12}}{f_2}\right)^{m-1} \qquad \text{(A-3)}$$

where the values of n, m, f_1 and f_2 are obtained from curve-fitting, unidirectional, experimental data and may vary with temperature. It is assumed that in the longitudinal direction, the non-linear part of the strain component is zero:

$$\varepsilon_{11}^{"} = 0 \ . \qquad \text{(A-4)}$$

The relationships between the non-linear parts of the strain components and the stress components for cases of combined transverse-extension and in-plane-shear stresses are determined by using a generalization of J_2 (ref. A-1) theory in addition to the requirement that these relationships reduce to equations (A-3) for uniaxial states of stress. The resulting equations are:

$$\varepsilon_{22}^{"} = \frac{\sigma_{22}}{\varepsilon_{22(T)}} \left(\frac{\sigma_{22}}{f_1}\right)^2 + \left(\frac{\sigma_{12}}{f_2}\right)^2 \Bigg)^{\frac{n-1}{2}}$$

$$\varepsilon_{12}^{"} = \frac{\sigma_{12}}{2G_{12(T)}} \left(\frac{\sigma_{22}}{f_1}\right)^2 + \left(\frac{\sigma_{12}}{f_2}\right)^2 \Bigg)^{\frac{m-1}{2}} . \qquad \text{(A-5)}$$

Equations (A-2) and (A-5) comprise the total non-linear, stress-strain relationship for the laminae.

The governing equations are formulated so that the three stress components in each lamina are the unknowns. Thus, for an N-layered laminate, the problem is formulated in terms of 3N unknowns. To obtain solutions, 3N equations are then required, and these equations consist of three equilibrium equations and 3(N-1) compatibility equations satisfying strain compatibility between adjacent laminae. The three equations of equilibrium for a laminate under a combined state of stress are:

$$\sum_{k=1}^{N} \sigma_{11}^{(k)} t_k = N_{11}$$

$$\sum_{k=1}^{N} \sigma_{22}^{(k)} t_k = N_{22} \qquad \text{(A-6)}$$

$$\sum_{k=1}^{N} \sigma_{12}^{(k)} t_k = N_{12}$$

where N_{11}, N_{22} and N_{12} are the applied stress resultants, t_k is the thickness of the kth lamina, and subscripts 1 and 2 denote the laminate axes. The 3(N-1) equations of strain compatibility are:

$$\varepsilon_{11}^{(k)} = \varepsilon_{11}^{(k-1)}$$

$$\varepsilon_{22}^{(k)} = \varepsilon_{22}^{(k-1)} \qquad \text{(A-7)}$$

$$\varepsilon_{12}^{(k)} = \varepsilon_{12}^{(k-1)}$$

$$k = 2,3,\ldots,N \ .$$

Equations (A-6) and (A-7) are the 3N equations required for the solution of the non-linear laminate problem. When the stress-strain relations given by equations (A-2), (A-4), and (A-5) are transformed to the laminate reference axes and substitute into equations (A-7), the governing equations can be expressed in functional form as:

$$F_k\ (\sigma_1,\ \sigma_2,\ \ldots,\ \sigma_1^2,\ \ldots) = 0 \qquad \text{(A-8)}$$

$$k = 1,\ 2,\ \ldots,\ 3N\ .$$

Method of Solution

Solutions of equations (A-8) for the 3N stress components are obtained by employing a Newton-Raphson iterative scheme. The functions F_k are first expanded in Taylor series about an approximate set of initial stresses, σ_j°. Considering only the first order terms of these series:

$$F_k = F_k^\circ + \left.\frac{\partial F_k}{\partial \sigma_j}\right|_{\sigma_j^\circ} \cdot \Delta\ \sigma_j$$

$$j,k = 1,\ 2,\ \ldots,\ 3N\ . \qquad \text{(A-9)}$$

By writing, $\Delta\ \sigma_j = \sigma_j - \sigma_j^\circ$, where σ_j are the solution values, equations (A-9) can be rewritten to give:

$$\sigma_j = \sigma_j^\circ - \frac{\partial F_k}{\partial \sigma_j} \cdot F_k^\circ$$

$$j,k = 1,\ 2,\ \ldots,\ 3N\ . \qquad \text{(A-10)}$$

For clarity, the notation in equations (A-10) is, in expanded form:

$$\sigma_j = \begin{Bmatrix} \sigma_1 \\ \sigma_2 \\ \cdot \\ \cdot \\ \cdot \\ \sigma_{3N} \end{Bmatrix} \tag{A-11}$$

$$\sigma_j^\circ = \begin{Bmatrix} \sigma_1^\circ \\ \sigma_2^\circ \\ \cdot \\ \cdot \\ \cdot \\ \sigma_N^\circ \end{Bmatrix} \tag{A-12}$$

$$F_k^\circ = \begin{Bmatrix} F_1^\circ \\ F_2^\circ \\ \cdot \\ \cdot \\ \cdot \\ F_N^\circ \end{Bmatrix} \tag{A-13}$$

and,

$$\left[\frac{\partial F_k}{\partial \sigma_j}\right]_{\sigma_j^\circ} = \begin{bmatrix} \frac{\partial F_1}{\partial \sigma_1} & \frac{\partial F_1}{\partial \sigma_2} \cdots \\ \frac{\partial F_2}{\partial \sigma_1} & \frac{\partial F_2}{\partial \sigma_2} \cdots \\ \cdot & \\ \cdot & \\ \cdot & \end{bmatrix}_{\sigma_j = \sigma_j^\circ} . \tag{A-14}$$

The solution for σ_j in equation (A-10) may be taken as the approximate, initial stress values for the next iteration step, and this process repeated until a result is obtained within some desired accuracy. After the stresses are obtained and transformed to the laminae natural axes, the corresponding laminae strains are determined from equations (A-1), (A-2), and (A-5).

Computer Program

The flow chart for the computer program is shown in figure A-1. The major sections of the program are the formation of the governing equations, the Newton-Raphson solution procedure and the failure checks.

Using the computer program notation, the governing equations take the form:

$$[A] \cdot \overline{SG} + \overline{B} = \overline{SGO} \qquad \text{(A-15)}$$

where $\overline{SG}$ and $\overline{SGO}$ are the stress solution vector and the applied stress vector, respectively. A is a matrix of constant elements which are the coefficients of the linear terms in the solution, and $\overline{B}$ is a vector containing the non-linear terms in the solution. The set of equations (A-15) are equivalent to equations (A-8). If in equation (A-15) the vector $\overline{B}$ is set to zero, the resulting equation:

$$[A] \cdot \overline{SG} = \overline{SGO} \qquad \text{(A-16)}$$

is the linear laminate solution. The stress vector, $\overline{SG}$, as determined from equation (A-16) is taken as the initial approximation for the stress vector in the Newton-Raphson procedure.

For the Newton-Raphson procedure, it is necessary to formulate the derivative of $([A] \cdot \overline{SG} + \overline{B})$ in equation (A-15) with respect to σ_j as well as the vector:

$$\overline{DC} = ([A] \cdot \overline{SGO} + \overline{B} - \overline{SGO}) . \qquad \text{(A-17)}$$

The vector $\overline{DC}$ corresponds to the vector $\overline{F_f^o}$ in equation (A-10), and an explicit evaluation of $\overline{DC}$ is obtained by using the current, approximate value for the solution stress vector, $\overline{SC}$. The derivative of $([A] \cdot \overline{SG} + \overline{B})$ is designated $\overline{DB}$ in the computer program, and is equivalent to the matrix $(\partial F_k / \partial \sigma_j)\sigma_j^o$ in equation (A-10). An explicit evaluation of $\overline{DB}$ is also obtained by using the current, approximate value for the solution stress vector, $\overline{SG}$.

In the program, the external loading is applied in increments. The approximate solution stress vector for the first load increment and the first Newton-Raphson iteration is determined from equation (A-16). For the second and third load increments, the approximate solution stress vectors for the first iteration are taken as the final solution stress vectors from the previous increments. Solutions for subsequent load increments are initiated by the following algorithm:

$$(SG_{i+1})_{INITIAL} = (SG_i)_{FINAL} * (FACTOR)$$

$$(FACTOR) = \frac{i\ (i-2)}{(i-1)^2} \frac{(SG_i)_{FINAL} - (SG_{i-1})_{FINAL}}{(SG_i)_{FINAL}} . \qquad \text{(A-18)}$$

The convergence and divergence criteria employed in the program are contained in the following expressions:

$$\left| (SG_{i+1} - SG_i)/SG_i \right| \leq \varepsilon$$

$$\left| (SG_{i+1} - SG_i)/SG_i \right| \geq \lambda \qquad \text{(A-19)}$$

where SG_i and SG_{i+1} are the solution vectors obtained from the ith and i+1th iterations. Usually values of 10^{-3} and 10^{+4} are taken for ε and λ, respectively. However, the other values may be input as data to the program. In addition, the maximum number of iterations to be allowed is input as data. 10 iterations have been found to be sufficient for most problems.

The program contains three failure criteria: maximum strain, maximum stress, and a quadratic interaction criterion. After a solution is obtained for each load increment, any or all of these failure criteria may be applied to check for laminae failure.

The maximum stress and maximum strain failure criteria check, respectively, the laminae stress or strain values in the fiber, and transverse fiber directions against the material allowables. These allowables are input to the program as data. The quadratic criterion is given by:

$$A_{11}\sigma_{LL}^2 + A_{22}\sigma_{TT}^2 + A_{44}\sigma_{LT}^2 + A_{12}\sigma_{LL}\sigma_{TT} + B_1\sigma_{LL} + B_2\sigma_{TT} = 1 \qquad \text{(A-20)}$$

where the coefficients are functions of the allowable stress:

$$A_{11} = \frac{1}{F_L^t F_L^c} \qquad B_{11} = \frac{1}{F_L^t} - \frac{1}{F_L^c}$$

$$A_{22} = \frac{1}{F_T^t F_T^c} \qquad B_{22} = \frac{1}{F_T^t} - \frac{1}{F_T^c} \qquad \text{(A-21)}$$

$$A_{44} = \frac{1}{(F^s)^2} \; .$$

F_L^t and F_L^c are the allowable tension and compression stresses in the longitudinal direction, F_T^t and F_T^c are the allowable tension and compression stresses in the transverse direction, and F^s is the allowable shear stress. The coefficient A_{12} is input as data to the program, or a default null value is used.

If a failure criterion is satisfied at the end of a load increment, the program determines the failure load through linear interpolation. If all failure criteria are being checked, and not all indicate failure during the same load increment, the program continues loading until all criteria indicate failure.

It is possible to input the experimental values of the elastic properties and strengths only at selected temperatures. If the analysis temperature is different from these temperatures, the properties are linearly interpolated at that temperature, and the governing equations set up.

TENOL PROGRAM USERS GUIDE

Program Description

The logic of the analysis code, simplified in the form of a flow chart, can be seen in figure A-1. The code was structured such that an existing code, NOLIN, could be used, with some modifications, to solve the non-linear equations with the Newton-Raphson iterative procedure. It consists of a main routine, an interface routine, and modified NOLIN. The equations are set up at the analysis temperature in the main routine using properties linearly interpolated in the interpolation routine. A more sophisticated interpolation scheme can be incorporated very easily into the program. The interface is a translation table to make modifications to the variables for compatibility with the modified NOLIN. All data are input in the form of a single NAMELIST called DATA.

Input Description

The initial data require a message of five cards of alphanumeric descriptive information describing the problem being solved and printed as a title on the output. These five cards may be left blank, but must be included ahead of the first NAMELIST deck in the data. This descriptive message is read only once at the beginning of the program execution. The multiple case feature of running successive computations is accomplished by supplying multiple NAMELIST data sets with the changed variables indicated.

The following is a description of the input variables required for execution of the program. Where appropriate, default or suggested values are indicated. The following data are supplied through NAMELIST "DATA":

Program Option Parameters

LTYPE: Load type sentinel
- LTYPE = 1: Load purely mechanical.
- LTYPE = 2: Load purely thermal.
- LTYPE = 3: Load thermomechanical.

Solution Accuracy Parameters

KSGM: Number of load increments; maximum is 50 increments.

IT: Maximum number of Newton-Raphson iterations; default if 100.

EPS: Convergence criteria for Newton-Raphson analysis; default value is 10^{-3}.

UPBD: Divergence criteria during Newton-Raphson analysis; default value is 20000.

INMT: Incrementation estimate method; default value is 2.

Laminate Description

NMAT: Number of different materials in the laminate; maximum is 5.

NLAY: Number of laminate layers; maximum is 20.

THICK(L): L = 1, NLAY; thickness of each layer.

THETA(L): Orientation of each layer in degrees.

MATYPE(L): Material kind of each layer.

Thermal Properties

SFT: Stress-free temperature.

NTEMPP: Number of temperatures at which data is input; maximum is 8.

TEMPP(I): I = 1, NTEMPP; temperatures at which data is input.

NALP: Number of temperatures at which $\Delta L/L$ points are input; maximum is 20.

ALPT(I): I = 1, NALP; number of temperatures at which $\Delta L/L$ points are input; maximum is 20.

Material Property Input

In this set of variables, I = 1, NTEMPP and J = 1, NMAT.

TE11(I,J): Material longitudinal modulus.

TE22(I,J): Transverse modulus.

TG12(I,J): Shear modulus.

TV12(I,J): Major Poisson's ratio.

TS11T(I,J): Longitudinal tensile strength.

TS11C(I,J): Longitudinal compressive strength.

TS22T(I,J): Transverse tensile strength.

TS22C(I,J): Transverse compressive strength.

TS12(I,J): In-plane shear strength.

TEP11T(I,J): Longitudinal tensile strain.

TEP11C(I,J): Longitudinal compressive strain.

TEP22T(I,J): Transverse tensile strain.

TEP22C(I,J): Transverse compressive strain.

TGAMA(I,J): In-plane shear strain.

TA12(I,J): Interaction term for quadratic interaction criteria; default value is 0.0.

TSTY(I,J): Ramberg-Osgood tension constant.

TSCY(I,J): Ramberg-Osgood compression constant.

TTY(I,J): Ramberg-Osgood shear constant.

TXM(I,J): Ramberg-Osgood shear exponent.

TXN(I,J): Ramberg-Osgood tension exponent.

For these variables, K = 1, NALP and L = 1, NMAT.

ALPHA1(K,L): $\Delta L/L$ value in the longitudinal direction.

ALPHA2(K,L): $\Delta L/L$ value in the transverse direction.

Applied Loading and Failure Criteria

SO11: Initial axial stress applied to laminate.

SO22: Initial transverse stress applied to laminate.

SO12: Initial shear stress applied to laminate.

IFCN: Failure criteria sentinel
IFCN = 1: Ultimate stress.
IFCN = 2: Ultimate strain.
IFCN = 3: Quadratic interaction.
IFCN = 4: All failure criteria.

STIFF: Ratio of final to initial laminate stiffness which constitutes failure due to stiffness reduction; default value is 0.10.

TEMP: Temperature at the end of the first load step.

STEMP: Temperature change in the subsequent load steps.

SMLT: Scaling factor yielding the subsequent load increments based on initial stress loads.

Calculation of Ramberg-Osgood Parameters

Ramberg-Osgood parameters are used to curve fit the experimental stress-strain data; the strain expressed as a polynomial of the stress. The code RAMOSG can be used for this purpose. Input to the program is in the form of engineering strains, and moduli, and is approximated by a least square curve fit of the type:

$$\varepsilon = \frac{\sigma}{E}\left(1 + \left(\frac{\sigma}{\sigma_y}\right)^{n-1}\right).$$

The program output is the strength parameter σ_y and the exponent n. There is an option that permits treating n as an input quantity with σ_y being calculated by the program. Input is in the form of a namelist INPUT. Data for different stress-strain curves can be input in namelists one after another if a set of Ramberg-Osgood parameters is required.

Input

EMOD: Engineering modulus (transverse or shear).

N: Total number of stress points input.

STRS(I): Ith stress point, naximum of 50.

STRN(I): Ith engineering strain point, maximum of 50.

IEXP: Ramberg-Osgood exponent.
IEXP = 0: if exponent is to be calculated by program.

REFERENCES

A-1. Hashin, Z., Bagchi, D., and Rosen, B. W., "Non-linear Behavior of Fiber Composite Laminates," NASA CR-2313, April 1974.

A-2. Kibler, J. J., "NOLIN - A Non-linear Laminate Analysis Program," NASA CR-2410, February 1975.

APPENDIX B

STRESS RELAXATION IN LAMINATES

This section gives in detail the analysis procedure followed to determine the characteristic time for stress relaxation in a laminate, given the unidirectional lamina behavior. It consists of developing the plane stress-strain relations in the form of hereditary integrals, taking their Laplace transforms and applying lamination theory. The viscoelastic behavior has to be modeled from experimental data and lamination theory results back transformed into the time domain. Such an analysis is conducted for a quasi-isotropic $[0/90/\pm45]_s$ laminate subject to a pure thermal loading.

In the $[0/90/\pm45]_s$ laminate, the thermal loading does not induce any thermal shear stresses or strains in each ply. The state of stress or strain is greatly simplified due to various symmetries. Due to the absence of shear, the unidirectional stress-strain relation for the unidirectional lamina becomes:

$$\varepsilon_{11} = \frac{\sigma_{11}}{E_A} - \frac{\nu_A}{E_A}\ \sigma_{22} + \alpha_A(\phi_o-\phi_c)$$

$$\varepsilon_{22} = -\frac{\nu_A}{E_A}\ \sigma_{11} + \frac{\sigma_{22}}{E_T} + \alpha_T(\phi_o-\phi_c). \qquad \text{(B-1)}$$

All the moduli in the above plane stress relations are constant in time. For the viscoelastic analysis, the axial modulus and Poisson's ratio can be assumed to be constant in time. If α_A and α_T are assumed to be constant, and there is viscoelastic behavior only in the transverse direction, then the above equations can be used to express the time dependent equations using hereditary integrals. If the relaxation process is defined to begin at time zero at temperature ϕ_o, the viscoelastic relations for time dependent stresses become:

$$\varepsilon_{11}(t) = \frac{\sigma_{11}}{E_A}(t) - \frac{\nu_A}{E_A}\ \sigma_{22}(t) + \alpha_A \Delta\phi\ H(t)$$

(B-2)

$$\varepsilon_{22}(t) = -\frac{\nu_A}{E_A}\ \sigma_{11}(t) + \ell_T(t)\sigma_{22}(o) + \int_o^t \ell_T(t-\tau)\ \frac{d\sigma_{22}}{d\tau}\ d\tau + \alpha_T \Delta\phi\ H(t)$$

where $e_T(t)$ is the creep compliance and H(t) the Heaviside unit step function.

The Laplace transform of a function f(t) is defined as:

$$\hat{f}(s) = \int_0^\infty f(t)e^{-st}dt. \qquad \text{(B-3)}$$

Transforming these equations using this definition results in:

$$\hat{\varepsilon}_{11}(s) = \frac{\hat{\sigma}_{11}(s)}{E_A} - \frac{\nu_A}{E_A}\ \hat{\sigma}_{22}(s) + \alpha_A \Delta\phi\ \frac{1}{s}$$

(B-4)

$$\hat{\varepsilon}_{22}(s) = -\frac{\nu_A}{E_A}\ \hat{\sigma}_{22}(s) + s\hat{e}_T(s)\hat{\sigma}_{22}(s) + \alpha_A \Delta\phi\ \frac{1}{s}\ .$$

Now:

$$s\hat{e}_T(s) = \frac{1}{s\hat{E}_T(s)} \qquad E_T \text{ - relaxation modulus}$$

$$\therefore\ \hat{\varepsilon}_{22}(s) = -\frac{\nu_A}{E_A}\ \hat{\sigma}_{11}(s) + \frac{\hat{\sigma}_{22}(s)}{s\hat{E}_T(s)} + \alpha_A \Delta\phi\ \frac{1}{s}\ .$$

Solving for $\hat{\sigma}_{11}$ and $\hat{\sigma}_{22}$:

$$\hat{\sigma}_{11} = \frac{1}{1 - \nu_A^2 s \frac{\hat{E}_T}{E_A}} \{(E_A \hat{\varepsilon}_{11} + \nu_A s \hat{E}_T \hat{\varepsilon}_{22}) - \frac{\Delta\phi}{s} (\alpha_A E_A + \nu_A \alpha_T s \hat{E}_T)\}$$

$$\hat{\sigma}_{22} = \frac{1}{1 - \nu_A^2 s \frac{\hat{E}_T}{E_A}} \{(\nu_A s \hat{E}_T \hat{\varepsilon}_{11} + s \hat{E}_T \hat{\varepsilon}_{22}) - \frac{\Delta\phi}{s} (\alpha_T + \nu_A \alpha_A) s \hat{E}_T\}. \quad \text{(B-5)}$$

These are the viscoelastic stress-strain relations for any lamina in the $[0/90/\pm45]_s$ laminate. These have to be transformed into the laminate coordinate system using the usual tensor transformations. Since the shear stresses are zero, these become:

$$^k\sigma_{11} = \sigma_{11}^k \cos^2\theta_k + \sigma_{22}^k \sin^2\theta_k$$

$$^k\sigma_{22} = \sigma_{11}^k \sin^2\theta_k + \sigma_{22}^k \cos^2\theta_k \quad \text{(B-6)}$$

where

$^k\sigma_{ij}$ - stresses with laminate coordinates

σ_{ij}^k - stresses with material coordinates

θ_k - orientation of the kth layer.

These relations are used to transform the stresses in each lamina:

$$
\begin{aligned}
{}'\sigma_{11} &= \sigma'_{11} & {}'\sigma_{22} &= \sigma'_{22} \\
{}^2\sigma_{11} &= \sigma^2_{22} & {}^2\sigma_{22} &= \sigma^2_{11} \\
{}^3\sigma_{11} &= \tfrac{1}{2}\,(\sigma^3_{11}+\sigma^3_{22}) = {}^3\sigma_{22} \\
{}^4\sigma_{11} &= \tfrac{1}{2}\,(\sigma^4_{11}+\sigma^4_{22}) = {}^4\sigma_{22}.
\end{aligned}
\qquad \text{(B-7)}
$$

Equilibrium requires that for plies of the thickness the equilibrium equations become:

$$\sum_{k=1}^{n} \{{}^k\sigma_{ij}\}h^k = \bar{\sigma}_{ij}h = 0. \qquad \text{(B-8)}$$

$$\tfrac{1}{4}\,{}'\sigma_{11} + \tfrac{1}{4}\,{}^2\sigma_{11} + \tfrac{1}{4}\,{}^3\sigma_{11} + \tfrac{1}{4}\,{}^4\sigma_{11} = 0$$

$$\tfrac{1}{4}\,{}'\sigma_{22} + \tfrac{1}{4}\,{}^2\sigma_{11} + \tfrac{1}{4}\,{}^3\sigma_{22} + \tfrac{1}{4}\,{}^4\sigma_{22} = 0$$

$$\therefore\quad \sigma'_{11} + \sigma^2_{22} + \tfrac{1}{2}\,(\sigma^3_{11}+\sigma^3_{22}) + \tfrac{1}{2}\,(\sigma^4_{11}+\sigma^4_{22}) = 0$$

$$\text{and}\quad \sigma'_{22} + \sigma^2_{11} + \tfrac{1}{2}\,(\sigma^3_{11}+\sigma^3_{22}) + \tfrac{1}{2}\,(\sigma^4_{11}+\sigma^4_{22}) = 0.$$

Since all the laminae are made from the same material, in the material coordinate system:

$$\sigma'_{11} = \sigma^2_{11} = \sigma^3_{11} = \sigma^4_{11} \tag{B-9}$$

and

$$\sigma'_{22} = \sigma^2_{22} = \sigma^3_{22} = \sigma^4_{22}. \tag{B-10}$$

Substituting these equalities in the equilibrium equations results in:

$$\sigma'_{11} + \sigma'_{22} + \frac{1}{2}(\sigma'_{11}+\sigma'_{22}) + \frac{1}{2}(\sigma'_{11}+\sigma'_{22}) = 0$$

i.e. $\sigma'_{11} + \sigma'_{22} = 0.$

Also:

$$\varepsilon'_{11} = \varepsilon^2_{11} = \varepsilon^3_{11} = \varepsilon^4_{11} = \varepsilon_{11} \tag{B-11}$$

and

$$\varepsilon'_{22} = \varepsilon^2_{22} = \varepsilon^3_{22} = \varepsilon^4_{22} = \varepsilon_{22}. \tag{B-12}$$

In the laminate coordinates the strains in all the layers are equal. i.e.:

$$'\varepsilon_{11} = {}^2\varepsilon_{11} = {}^3\varepsilon_{11} = {}^4\varepsilon_{11} \tag{B-13}$$

and

$$'\varepsilon_{22} = {}^2\varepsilon_{22} = {}^3\varepsilon_{22} = {}^4\varepsilon_{22}. \tag{B-14}$$

The strain transformation equations for this laminate are:

$$^{k}\varepsilon_{11} = \varepsilon_{11}^{k}\cos^{2}\theta_{k} + \varepsilon_{22}^{k}\sin^{2}\theta_{k}$$

$$^{k}\varepsilon_{22} = \varepsilon_{11}^{k}\sin^{2}\theta_{k} + \varepsilon_{22}^{k}\cos^{2}\theta_{k}.$$

For the $[0/90/\pm45]_{s}$ laminate, the strains in the laminate coordinates are:

$$^{'}\varepsilon_{11} = \varepsilon_{11}^{'} = \varepsilon_{11} \qquad ^{'}\varepsilon_{22} = \varepsilon_{22}^{'} = \varepsilon_{22}$$

$$^{2}\varepsilon_{11} = \varepsilon_{22}^{2} = \varepsilon_{22} \qquad ^{2}\varepsilon_{22} = \varepsilon_{11}^{2} = \varepsilon_{11}.$$

Substituting these in

$$\varepsilon_{11} = \varepsilon_{22} = \varepsilon.$$

Taking Laplace transforms of

$$\hat{\sigma}_{11} + \hat{\sigma}_{22} = 0$$

and

$$\hat{\varepsilon}_{11} = \hat{\varepsilon}_{22} = \hat{\varepsilon}.$$

The unidirectional viscoelastic stress-strain relations then simplify to:

$$(1-\nu_A^2 s\frac{\hat{E}_T}{E_A})\hat{\sigma}_{11} = (E_A+\nu_A s\hat{E}_T)\hat{\varepsilon} - \frac{\Delta\phi}{s}(\alpha_A E_A+\nu_A\alpha_T s\hat{E}_T)$$

$$(1-\nu_A^2 s\frac{\hat{E}_T}{E_A})\hat{\sigma}_{22} = (\nu_A s\hat{E}_T+s\hat{E}_T)\hat{\varepsilon} - \frac{\Delta\phi}{s}(\alpha_T+\nu_A\alpha_A)s\hat{E}_T.$$

Substituting into

$$\hat{\varepsilon} = \frac{\Delta\phi}{s}\{\alpha_A + \frac{(\alpha_T-\alpha_A)(1+\nu_A)}{1 + 2\nu_A + \frac{E_A}{s\hat{E}_T}}\} \qquad \text{(B-15)}$$

and the stresses:

$$\hat{\sigma}_{11} = \frac{\Delta\phi}{s} \times \frac{E_A(\alpha_T-\alpha_A)}{1 + 2\nu_A + \frac{E_A}{s\hat{E}_T}} = \frac{\Delta\phi}{s} \times \frac{E_A(\alpha_T-\alpha_A)}{1 + 2\nu_A + E_A s\hat{e}_T}$$

$$\hat{\sigma}_{22} = -\hat{\sigma}_{11}. \qquad \text{(B-16)}$$

The stresses have now been solved for in the 's' plane in terms of the constants E_A, α_A, α_T, $\Delta\phi$ and ν_A and the transform time dependent compliance. This is obtained from experimental data, and is different for different material. It can be obtained from curve fitting the data with a series of exponential functions, or modeled with various spring-dashpot models. The model parameters are then determined experimentally. The exact back transformation of the stresses into real time may not be possible for some of the forms of $e_T(t)$ and approximate numerical techniques may have to be used.

For the sake of demonstration of the methodology, a simple Maxwell model was assumed for obtaining $e_T(t)$. The stresses can then be easily obtained by back transforming (eqn. B-
A Maxwell material can be characterized by the constitutive relation:

$$\varepsilon_{22} = \frac{\sigma_{22}}{E_T} + \frac{\dot{\sigma}_{22}}{\eta_T} \cdot \qquad \text{(B-17)}$$

Applying Laplace transformation, this equation becomes:

$$s\hat{\varepsilon}_{22} = s\frac{\hat{\sigma}_{22}}{E_T} + \frac{\hat{\sigma}_{22}}{\eta_T} = \hat{\sigma}_{22}\left(\frac{s}{E_T} + \frac{1}{\eta_T}\right.$$

$$\therefore \quad \hat{\varepsilon}_{22} = \left(\frac{1}{E_T} + \frac{1}{s\eta_T}\right)\hat{\sigma}_{22} = s\hat{e}_T\hat{\sigma}_{22}$$

$$\therefore \quad s\hat{e}_T = \frac{1}{E_T} + \frac{1}{s\eta_T} = \frac{1}{E_T}\left(1 + \frac{E_T}{s\eta_T}\right).$$

Substituting t_r, the characteristic time, defined as:

$$t_r = \frac{\eta_T}{E_T}$$

$$s\hat{e}_T = \frac{1}{E_T}\left(1 + \frac{1}{st_r}\right). \qquad \text{(B-18)}$$

Introducing this form of the creep compliance in equation

$$\hat{\sigma}^{k}_{22} = - \frac{\Delta\phi}{s} \times \frac{E_A(\alpha_T-\alpha_A)}{1 + 2\nu_A + \frac{E_A}{E_T}(1 + \frac{1}{st_r})}$$

$$= - \Delta\phi \frac{E_A(\alpha_T-\alpha_A)}{s(1+2\nu_A+ \frac{E_A}{E_T}) + \frac{E_A}{E_T t_r}}$$

$$= - \Delta\phi \frac{E_A(\alpha_T-\alpha_A)}{1 + 2\nu_A + \frac{E_A}{E_T}} \times \frac{1}{s + \frac{E_A/E_T}{1 + 2\nu_A + E_A/E_T} \times \frac{1}{t_r}}$$

Back transforming, the stress response in real time becomes:

$$\sigma^{k}_{22}(t) = - \Delta\phi \frac{E_A(\alpha_T-\alpha_A)}{1 + 2\nu_A + \frac{E_A}{E_T}} \exp \{- \frac{t}{t_r} \times \frac{E_A/E_T}{1 + 2\nu_A + E_A/E_T}\}$$

$$= - \Delta\phi \frac{E_A(\alpha_T-\alpha_A)}{1 + 2\nu_A + \frac{E_A}{E_T}} \exp \{- \frac{t}{t^*_r}\} \qquad \text{(B-19)}$$

$$t^*_r = t_r \times \frac{1 + 2\nu_A + E_A/E_T}{E_A/E_T}$$

$$= t_r \times (1 + \frac{(1+2\nu_A)E_T}{E_A})$$

$\therefore \quad t^*_r > t_r.$

Laminate stresses, therefore, relax at a slower rate than the unidirectional lamina stresses. The above methodology demonstrated the procedure to be followed for obtaining the relaxation behavior of the stresses in a laminate. In general, the application of lamination theory in the transformed plane is much more complicated due to the presence of shear moduli. The layers are also at different angles and the transformation of the stresses and strains from the material to the laminate coordinates results in further complications. As explained earlier, the inversion also has to be done numerically, and the stresses plotted against time, to determine the characteristic relaxation times. A simpler approach could be the assumption of quasi-elastic behavior. The compliance and moduli are then simple reciprocals of each other, and the stresses can be obtained by direct integration. Such an approach has been followed by Kibler (ref. B-1).

REFERENCE

B-1. Kibler, K. G., "Effects of Temperature and Moisture on the Creep Compliance of Graphite-Epoxy Composites," Reprint.

APPENDIX C

THERMAL CYCLING OF VISCOELASTIC LAMINATES

This section describes in some detail the formulation used for evaluation of the effects of stress relaxation during thermal cycling. It is merely to demonstrate a methodology, and many simplifying assumptions have been made to reduce the complexity of the resulting equations. This formulation is a modification of the analysis of viscoelastic effects made in reference C-1, and the detailed formulation can be found in that reference. The principal assumption is that the material behavior can be assumed to be linearly viscoelastic, and that the correspondence principal can be applied. Therefore, the stress and strain behavior in the Laplace transformed domain can be obtained by merely rewriting the elastic results with the operational modulus.

Viscoelastic behavior is temperature dependent, and hence, in making calculations at different temperatures in the thermal cycle, different properties have to be used. These calculations can be greatly simplified if the material can be characterized as thermorheologically simple. This assumption means that if the relaxation function of the material is plotted against time from experiments performed at a particular temperature, the material response in time at a different temperature can be obtained by merely shifting the relaxation function to the left or right along the time axis. For example, the response function at temperature ϕ can be obtained from the function at temperature ϕ_0 by shifting that curve by $a_T(\phi)$, figure C-1, or at temperature ϕ_2 by shifting the curve at ϕ_0 by $a_T(\phi_0)$. Thus the material can be completely characterized by a response function at some temperature, if the amount by which this curve needs to shifted at various temperatures is known, i.e. if the variation of the shift factor in temperature is known. That relaxation function is known as the master curve, and the temperature at which it is plotted, the reference temperature. The time for the function

to attain a certain value is temperature dependent, so the master curve has to be drawn against 'reduced time' ζ, defined to be:

$$\zeta = \int_0^t \frac{d\lambda}{a_T[T(\lambda)]} \tag{C-1}$$

such that $E_T(\zeta) = E_T(t,\phi_0)$,

ϕ_0 = the reference temperature such that $a_T(\phi_0)=1$.

In the present analysis a cross-ply laminate subject to thermal cycling was modeled with lamination theory. A state of plane stress is assumed to exist and the lamina strain is assumed to be :

$$\varepsilon_{11} = \frac{\sigma_{11}}{E_A} + \frac{\nu_{12}}{E_A}\sigma_{22} + \alpha_A\Delta\phi$$

and (C-2)

$$\varepsilon_{22} = \nu_{12}\frac{\sigma_{11}}{E_A} + \frac{\sigma_{22}}{E_T} + \alpha_T\Delta\phi.$$

In a cross-ply laminate, subject to a pure thermal load, the state of stressand strain is simplified greatly by various symmetries. There is numerically only one stress and one strain to be solved from lamination theory, and the result for the stress is:

$$\sigma = \frac{E_A(\alpha_T-\alpha_A)\Delta\phi}{1 + 2\nu_A + E_A/E_T} = \frac{E_T(\alpha_T-\alpha_A)\Delta\phi}{1 + E_T/E_A^*} \tag{C-3}$$

where $E_A^* = \dfrac{E_A}{1 + 2\nu_A}$.

The axial modulus E_A and the Poisson's ratio and the expansion coefficients are assumed to be constant in time, so the only modulus that changes in time is E_T. Applying the correspondence principal to this equation, the stress behavior in the Laplace transformed plane can be written as:

$$\frac{\hat{\sigma}}{\alpha_T - \alpha_A} = \frac{\tilde{E}_T \Delta \hat{T}}{1 + \tilde{E}_T / E_A^*} \tag{C-4}$$

where the Laplace transformed stress $\hat{\sigma}$ is defined:

$$\hat{\sigma} = \int e^{-p\zeta} \sigma(\zeta) d\zeta \tag{C-5}$$

and $\tilde{E}_T$ the operation modulus as $\tilde{E}_T = p\hat{E}_T$.

Let a modulus function be defined such that:

$$p\hat{f}(p) = \frac{\tilde{E}_T}{1 + \tilde{E}_T / E_A^*} \tag{C-6}$$

for a unit step change in the temperature $\Delta\phi$, represented by the Heaviside function $H(\zeta)$; then

$$\frac{\hat{\sigma}}{\alpha_T - \alpha_A} = p\hat{f}(p)\Delta\hat{\phi} = \hat{f}(p) \tag{C-7}$$

or

$$\frac{\sigma(\zeta)}{\alpha_T - \alpha_A} = \hat{f}(\zeta) \quad \text{by inversion.} \tag{C-8}$$

For an arbitrary temperature history (C-7) can be generalized to:

$$\frac{\sigma(\zeta)}{\alpha_T - \alpha_A} = \int_0^{\zeta} f(\zeta-\zeta') \frac{d}{d\zeta'} [\Delta T(\zeta')] d\zeta' \ . \qquad \text{(C-9)}$$

Hence, if $f(\zeta)$ can be obtained, the stress can be calculated by direct integration. If the 0° ply is assumed to be rigid with respect to the 90° ply (i.e. $E_A >> E_T$) equation (C-6) reduces to $f(\zeta) = E_T(\zeta)$.

The function $f(\zeta)$ is calculated as follows. Let:

$$f(\zeta) = E_T^{\circ} \, g(\zeta) \qquad \text{(C-10)}$$

where $g(\zeta) = \dfrac{h(\zeta)}{1 + h(\zeta)}$

$$h(\zeta) = \frac{E_T(\zeta)}{E_T^{\circ}}$$

E_T° = a constant chosen such that $h(0) = 1$, and $\beta = \dfrac{E_T^{\circ}}{E_A^{*}}$.

Substituting (C-10) in (C-9):

$$\frac{\sigma(\zeta)}{E_T^{\circ}(\alpha_T-\alpha_A)} = \int_0^{\zeta} g(\zeta-\zeta') \frac{d[\Delta T(\zeta')]}{d\zeta'} d\zeta \ . \qquad \text{(C-11)}$$

Now $h(\zeta)$ is the normalized relaxation modulus master curve. The real problem is obtaining this curve from experimental data that are in terms of the creep compliance. There are various methods to do this, like the direct method (ref. C-2) or by the quasi-elastic method (ref. C-3). In this report the latter was used because of its simplicity. The relaxation modulus by this method is just the reciprocal of the creep compliance.

The integral in (C-11) is evaluated as follows. The experimental data for the variation of the shift factor a_T with temperature has to be curve fitted. As seen in figure C-2, a linear variation of log a_T can be assumed, i.e.

$$a_T(\phi) = e^{b(\phi-\phi_0)} \quad . \tag{C-12}$$

The temperature time relationship is piece-wise linear in time intervals t_i, ... t_i, t_{i+1} for the laminate (fig. C-2). For $t_i < t < t_{i+1}$:

$$\frac{dT}{dt} = \tan \phi_i = C_i = \frac{T_{i+1} - T_i}{t_{i+1} - t_i} \tag{C-13}$$

$$T(t) = T_i + C_i(t-t_i) \tag{C-14}$$

$$\Delta T(t) = T_i - T_i + C_i(t-t_i) \quad . \tag{C-15}$$

Use of equations (C-2), (C-12), (C-14), and (C-15) yield:

$$\zeta(t) = \int_0^{t_i} \frac{dt'}{a_T[T(t'(]} + \int_{t_i}^{t} \frac{dt'}{a_T[T(t')]} \tag{16a}$$

$$= \zeta_i + \frac{1}{bC_i} \left[\frac{1}{a_T[T(t)]} - \frac{1}{a_T(T_i)}\right] ; \; C_i \neq 0 \tag{16b}$$

$$= \zeta_i + \frac{t - t_i}{a_T(T_i)} \qquad ; \; C_i = 0. \tag{16c}$$

Also:

$$\zeta_i = \zeta(t_1) = 0 \tag{17a}$$

$$\zeta_i = \zeta(t_i) = \sum_{n=1}^{i-1} d_n \qquad ; \; i > 1 \tag{17b}$$

$$d_n = \frac{1}{bC_n} \left(\frac{1}{a_T(T_{n=1})} - \frac{1}{a_T(T_n)}\right) ; \; C_n \neq 0 \tag{17c}$$

$$d_n = \frac{t_{n+1} - t_n}{a_T(T_n)} \qquad ; \; C_n = 0. \tag{17d}$$

For $\zeta_i < \zeta < \zeta_{i+1}$:

$$\frac{d\Delta T(\zeta)}{d\zeta} = C_i \, a_T \, [T(\zeta)]. \qquad \text{(C-18)}$$

Substitution of (C-18) in (C-11) and use of (16a) yield:

$$\frac{\sigma_m(\zeta)}{E_m^{\circ}(\alpha_f - \alpha_m)} = S_i(\zeta) + \int_{\zeta}^{\zeta} g(\zeta - \zeta') C_i a_T [T(\zeta')] d\zeta' \qquad \text{(C-19a)}$$

$$\frac{\sigma_m(t)}{E_m'(\alpha_f - \alpha_m)} = S_i(t) + \int_{t_i}^{t} g[\zeta(t) - \zeta(t')] C_i dt' \qquad \text{(C-19b)}$$

for $t > t_i$ and $\zeta > \zeta_i$.

Also:

$$S_1(t) = 0 \qquad \text{(C-20a)}$$

$$S_1(t) = \sum_{n=1}^{i-1} e_n(t) \qquad ; \; i > 1 \qquad \text{(C-20b)}$$

$$e_n = \int_{\zeta_n}^{\zeta_{n+1}} g(\zeta - \zeta') C_i a_T [T(\zeta')] d\zeta' \; ; \; \zeta > \zeta_{n+1} \qquad \text{(C-20c)}$$

$$e_n = \int_{t_n}^{t_{n+1}} g[\zeta(t)-\zeta(t')]C_i dt' \quad ; \; t > t_{n+1}. \qquad \text{(C-20d)}$$

The integral in (C-11) can now be evaluated by numerical methods and use of (C-19b), (C-20b), and (C-20d).

REFERENCES

C-1. Kibler, J. J., Derby, E. A., Chatterjee, S. N., and Oscarson, J., "Structural Assessment of 3-D Carbon-Carbon Cylinders During Processing," AFML-TR-78-75, April 1978.

C-2. Schapery, R. A., "Stress Analysis of Viscoelastic Composite Materials," Composite Materials Workshop, Tsai, S. W., Halpin, J. C., and Pagano, N. J., editors, Technomic Publishing Company, 1968.

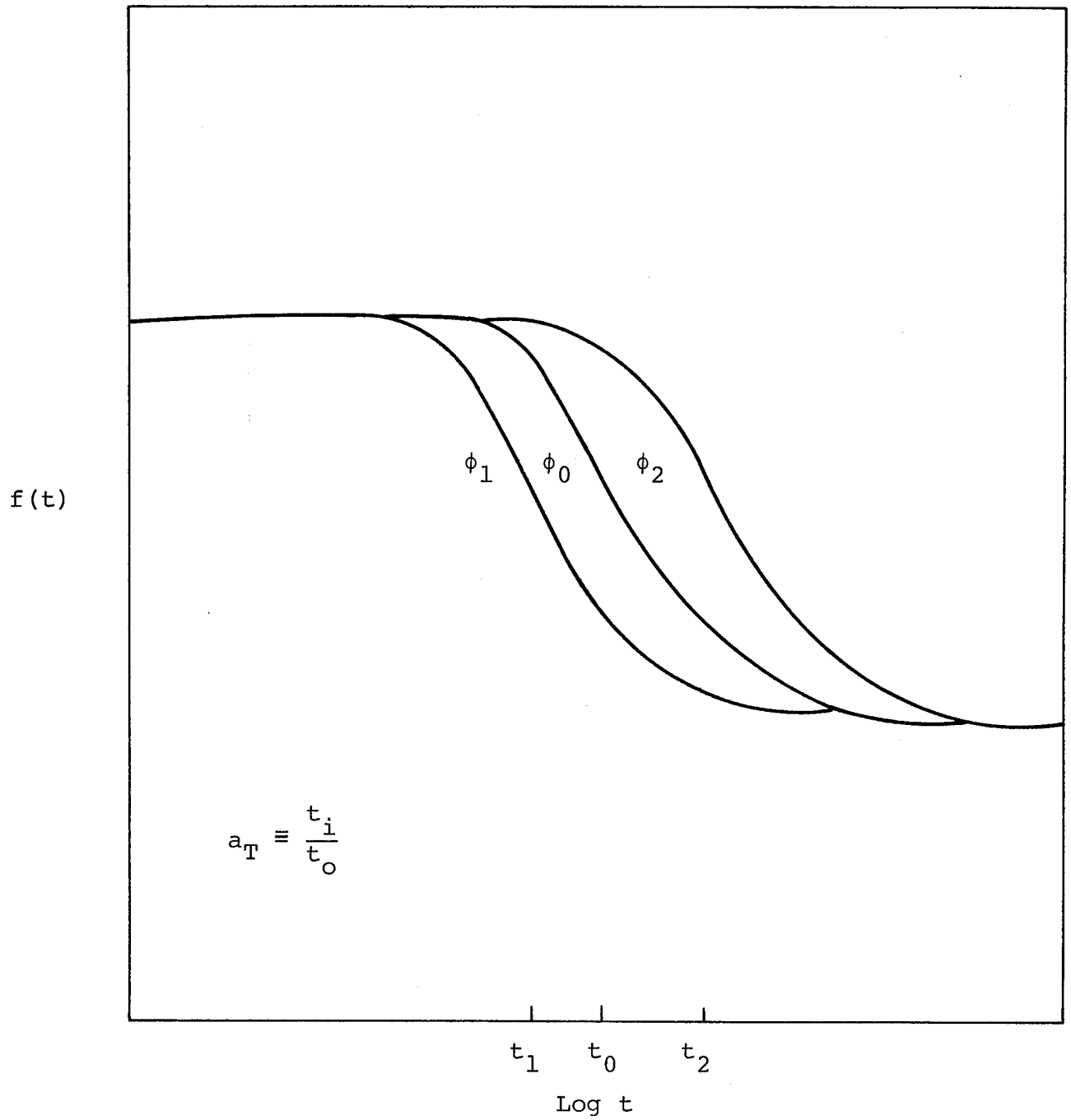

Figure C-1. Shift Factor

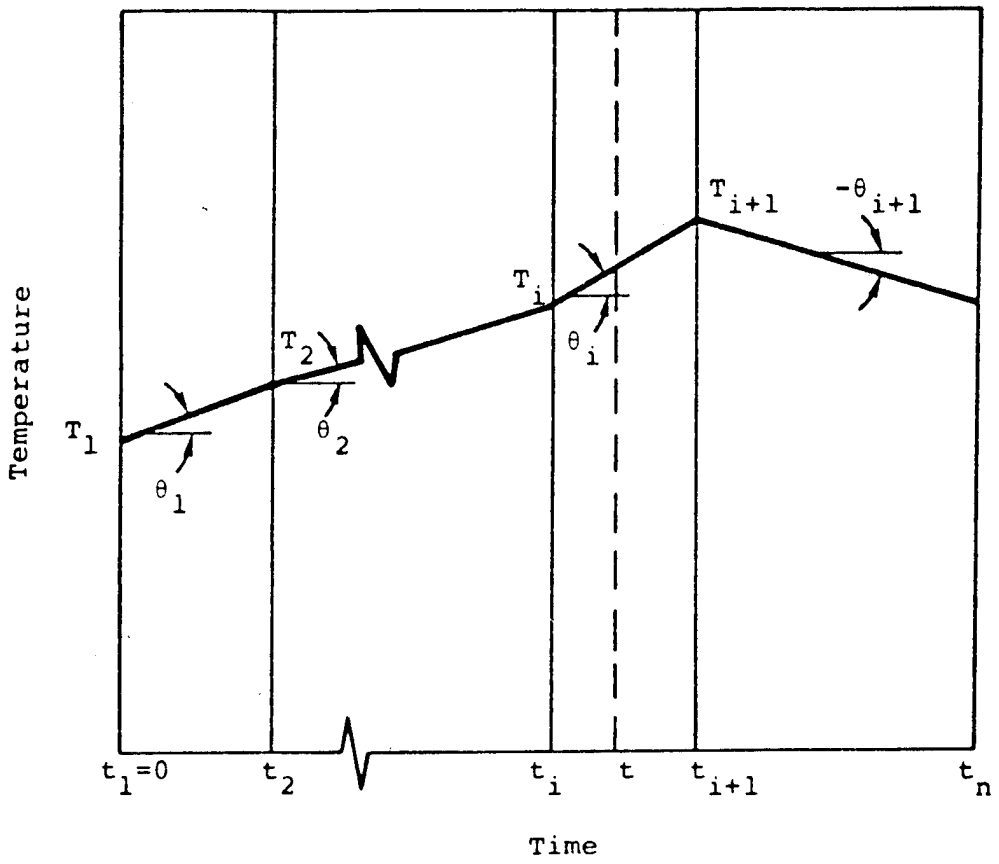

Figure C-2. Time-Temperature Curve

NASA Contractor Report 165753

Distribution List
NAS1-15841

	No. Copies
NASA Langley Research Center Hampton, VA 23665	
Attn: Report and Manuscript Control Office, Mail Stop 180A	1
J. G. Davis, Jr., Mail Stop 188A	6
H. Benson Dexter, Mail Stop 188A	1
P. A. Cooper, Mail Stop 190	1
H. M. Adelman, Mail Stop 243	1
Technology Utilization Office, Mail Stop 139A	1
NASA Ames Research Center Moffett Field, CA 94035	
Attn: Library, Mail Stop 202-3	1
Donald J. Graham, Mail Stop 227-2	1
NASA Dryden Flight Research Center Edwards, CA 93523	
Attn: Library	1
Dr. Eldon E. Kordes	1
NASA Goddard Space Flight Center Greenbelt, MD 20771	
Attn: Library	1
Jet Propulsion Laboratory 4800 Oak Grove Drive Pasadena, CA 91103	
Attn: Library, Mail 111-113	1
NASA Lyndon B. Johnson Space Center Houston, TX 77058	
Attn: JM6/Library	1
ES12/Leslie G. St. Leger	1
NASA John F. Kennedy Space Center Kennedy Space Center, FL 32899	
Attn: Library, NWSI-D	1
NASA Lewis Research Center 21000 Brookpark Road Cleveland, OH 44135	
Attn: Library, Mail Stop 60-3	1
Raymond F. Lark, Mail Stop 49-3	1
James R. Barber, Mail Stop 500-203	1
NASA Marshal Space Flight Center Marshall Space Flight Center, AL 35812	
Attn: AS61L/Library	1
EP13/Erich E. Engler	1

	No. Copies
National Aeronautics and Space Administration Washington, DC 20546 Attn: RTM-6/Leonard A. Harris	1
Air Force Flight Dynamics Laboratory Wright-Patterson Air Force Base, OH 45433 Attn: Philip Parmly, Code FBE	1
Directorate of Airframe Subsystems Engineering (ASNF) Systems Engineering Group Wright-Patterson Air Force Base, OH 45433 Attn: Dr. S. Tsai, Code MBM	1
Office, Chief of Research & Development Physical & Engineering Sciences Division Department of the Army Washington, DC 20310 Attn: Richard L. Ballard	1
Army Aviation Systems Command 12th and Spruce Streets St. Louis, MO 63166 Attn: J. Rickmeyer, AMCPM-HLS-T	1
U.S. Army Research and Technology Laboratories Fort Eustis Directorate (AVRADCOM) Fort Eustis, VA 23604 Attn: J. Shipley	1
U.S. Army Research and Technology Laboratories Structures Laboratory (AVRADCOM) NASA Langley Research Center Hampton, VA 23665 Mail Stop 266	1
Army Materials and Mechanics Research Center Watertown, MA 02172 Attn: Dr. E. Lenoe	1
Picatinny Arsenal Dover, NJ 07801 Attn: Charles Wright, Building 183, Materials Engineering Laboratory	1
Watervliet Arsenal Watervliet, NY 12189 Attn: F. W. Schmiedschoff	1
Department of the Navy Naval Air Systems Command Washington, DC 20360 Attn: Edwin M. Ryan, Code AIR-5302	1

	No. Copies
Naval Air Development Center Aero Structures Department Johnsville Warminster, PA 18974 Attn: J. J. Minecci, Code STD-9	1
Naval Research Laboratory Washington, DC 20390 Attn: J. A. Kies	1
National Bureau of Standards Washington, DC 20234 Attn: Leonard Mordfin, Engineering Mechanics Section	1
AVCO Corporation P. O. Box 210 Nashville, TN 37202 Attn: E. L. Anderson	1
The Boeing Company Commercial Airplane Group P. O. Box 3707 Seattle, WA 98124 Attn: John E. McCarty, Mail Stop 9k-23	1
The Boeing Company Vertol Division Morton, PA 19070 Attn: R. Pinckney	1
The Boeing Company Aerospace Group P. O. Box 3999 Seattle, WA 98124 Attn: D. K. Zimmerman	1
Bell Aerospace Company Post Office Box One Buffalo, NY 14240 Attn: F. M. Anthony	1
Bell Helicopter Company Box 482 Fort Worth, TX 76101 Attn: Herbert Zinberg, Advanced Engineering	1
Battelle Columbus Laboratories Metals & Ceramics Information Center 505 King Avenue Columbus, OH 43201 Attn: Robert T. Niehoff, Information Specialist	1

	No. Copies
General Dynamics Corporation Fort Worth Division P. O. Box 748 Fort Worth, TX 76101 Attn: Max Waddoups, MZ 2884	1
General Dynamics Corporation Convair Division San Diego, CA 92117 Attn: William H. Schaefer, Mail Zone 610-02 W. Wennhold, Mail Zone 646-00	1 1
General Electric Company Space Sciences Laboratory P. O. Box 8555 Philadelphia, PA 19101 Attn: David M. Purdy, Manager Vehicle & Electromechanical Engineering	1
Goodyear Aerospace Corporation Composite Products Engineering 1210 Massilon Road Akron, OH 44315 Attn: Louis W. Toth, D/562	1
Grumman Aerospace Corporation Bethpage, NY 11714 Attn: R. N. Hadcock, Advanced Composites, Plant 35 A. August, Advanced Development, Plant 35	1 1
Hughes Tool Company Aircraft Division Culver City, CA 90230 Attn: R. Wagner	1
IIT Research Institute 10 West 35th Street Chicago, IL 60616 Attn: Dr. R. H. Cornish	1
Lockheed Aircraft Corporation Lockheed-Georgia Company 86 South Cobb Drive Marietta, GA 30060 Attn: A. L. Cunningham, Director, ACIC, Dept. 72-26, Zone 28 W. E. Harvill, Dept. 72-26, Zone 28	1 1
Lockheed Aircraft Corporation Lockheed Missiles & Space Company P. O. Box 504 Sunnyvale, CA 94088 Attn: D. N. Yates, Dept. 81-12, Building 154	1
LTV Aerospace Corporation P. O. Box 5907 Dallas, TX 75222 Attn: Charles R. Foreman, Unit 2-53443	1

	No. Copies
Martin Marietta Corporation P. O. Box 179 Denver, CO 80201 Attn: John Lager	1
McDonnell Douglas Corporation Western Division 5301 Bolsa Avenue Huntington Beach, CA 92647 Attn: C. Y. Kam	1
McDonnell Douglas Corporation P. O. Box 516 St. Louis, MO 63166 Attn: Robert C. Goran, Dept. 2030, Building 1	1
Lockheed Aircraft Corporation Lockheed-California Company Burbank, CA 91503 Attn: John H. Wooley, Dept. 74-50, Building 85	1
McDonnell Douglas Corporation 3855 Lakewood Boulevard Long Beach, CA 90846 Attn: Dr. H. C. Schjelderup, CI-251, MS 1-18	1
Rockwell International Corporation Columbus Aircraft Division 4300 East 5th Avenue Columbus, OH 43216 Attn: R. W. Gehring, Dept. 71-522	1
Northrop Corporation 3901 West Broadway Hawthorne, CA 90250 Attn: C. Rosenkranz, Chief, Structures Research & Technology	1
United Aircraft Corporation Sikorsky Aircraft Division Stratford, CT 06497 Attn: Mel Rich	1
Stanford University Stanford, CA 94305 Attn: Professor Holt Ashley, Department of Aeronautics & Astronautics	1
TRW Systems One Space Park Redondo Beach, CA 90278 Attn: R. W. Vaughan	1
Union Carbide Corporation Carbon Products Division P. O. Box 6116 Cleveland, OH 44161 Attn: J. C. Bowman, Director, Research & Advanced Technology	1

	No. Copies
E. I. duPont de Nemours & Company Industrial Fibers Division Wilmington, DE 19898 Attn: Paul Langston	1
Rockwell International Corporation Space Division 12214 Lakewood Boulevard Downey, CA 90241 Attn: Jim Collipriest	1
Aeronautical Systems Division Wright-Patterson Air Force Base, OH 45433 Attn: Tom Bennett, ASD/ENFSA	1
The Boeing Company Boeing Commercial Airplane Division Mail Stop 77-21 Seattle, WA 98124 Attn: Stanley T. Harvey	1
NASA Scientific and Technical Information Facility 6571 Elkridge Landing Road Linthicum Heights, MD 21090	25 plus original
ARRADCOM Plastics Technical Evaluation Center Dover, NJ 07801 Attn: Alfred M. Anzalone, Bldg. 3401	1

1. Report No.	2. Government Accession No.	3. Recipient's Catalog No.
NASA CR 165753		

4. Title and Subtitle	5. Report Date
Thermomechanical Response of Gr/Pi Composites	March, 1981
	6. Performing Organization Code

7. Author(s)	8. Performing Organization Report No.
B. Walter Rosen, Aniruddha P. Nagarkar and Zvi Hashin	MSC TFR 1202/0207
	10. Work Unit No.

9. Performing Organization Name and Address	11. Contract or Grant No.
Materials Sciences Corporation Gwynedd Plaza II Bethlehem Pike Spring House, PA 19477	NAS1-15841
	13. Type of Report and Period Covered

12. Sponsoring Agency Name and Address	13. Type of Report and Period Covered
National Aeronautics & Space Administration Langley Research Center Hampton, VA 23665	Final Report 10/1/79 - 3/30/81
	14. Sponsoring Agency Code

15. Supplementary Notes

Langley Technical Representative: Dr. John Davis

16. Abstract

The effects of temperature changes upon the stresses and strains in composite laminates having carbon fibers in a polyimide matrix have been evaluated. The study treated composites having laminae in which there were non-linear stress-strain relations for stresses transverse to the fibers and for axial shear stresses. Material properties were considered to be temperature dependent. Separately, the effects of laminae viscoelastic response were also treated.

Recent experimental data for a carbon/polyimide composite material were utilized in the present analyses. The results suggest that, for this material, non-linearities due either to stress or time dependent effects do not appear to be of major practical importance for conventional high temperature composite structures. However, the effects of time dependent characteristics and temperature dependent properties can be of significance in understanding the behavior of dimensionally stable structures designed for long lifetimes.

17. Key Words (Suggested by Author(s))	18. Distribution Statement
Lamina non-linearity, Stress-interaction, Time Dependent, Temperature Dependent, Laminate Analysis, Graphite-polyimide, Dimensional Stability	Unclassified-Unlimited

19. Security Classif. (of this report)	20. Security Classif. (of this page)	21. No. of Pages	22. Price
Unclassified	Unclassified	106	

For sale by the National Technical Information Service, Springfield, Virginia 22161